



HAL
open science

The Solvation of Bromide Anion in Acetonitrile: A Structural Study Based on the Combination of Theoretical Calculations and X-ray Absorption Spectroscopy

Regla Ayala, Jose M. Martinez, Rafael R. Pappalardo, Adela Muñoz-Paez,
Enrique Sanchez Marcos

► To cite this version:

Regla Ayala, Jose M. Martinez, Rafael R. Pappalardo, Adela Muñoz-Paez, Enrique Sanchez Marcos. The Solvation of Bromide Anion in Acetonitrile: A Structural Study Based on the Combination of Theoretical Calculations and X-ray Absorption Spectroscopy. *Molecular Simulation*, 2007, 32 (12-13), pp.1035-1043. 10.1080/08927020601089064 . hal-00515008

HAL Id: hal-00515008

<https://hal.science/hal-00515008>

Submitted on 4 Sep 2010

HAL is a multi-disciplinary open access archive for the deposit and dissemination of scientific research documents, whether they are published or not. The documents may come from teaching and research institutions in France or abroad, or from public or private research centers.

L'archive ouverte pluridisciplinaire **HAL**, est destinée au dépôt et à la diffusion de documents scientifiques de niveau recherche, publiés ou non, émanant des établissements d'enseignement et de recherche français ou étrangers, des laboratoires publics ou privés.

The Solvation of Bromide Anion in Acetonitrile: A Structural Study Based on the Combination of Theoretical Calculations and X-ray Absorption Spectroscopy

Journal:	<i>Molecular Simulation/Journal of Experimental Nanoscience</i>
Manuscript ID:	GMOS-2006-0144.R1
Journal:	Molecular Simulation
Date Submitted by the Author:	26-Oct-2006
Complete List of Authors:	Ayala, Regla; Universidad de Sevilla, Quimica Fisica Martinez, Jose M.; Universidad de Sevilla, Quimica Fisica Pappalardo, Rafael R.; Universidad de Sevilla, Quimica Fisica Muñoz-Paez, Adela; Universidad de Sevilla, Quimica Inorganica e Instituto de Ciencia de Materiales-CSIC Sanchez Marcos, Enrique; Universidad de Sevilla, Quimica Fisica
Keywords:	MD Simulation, XANES spectrum, Interaction Potentials, Ab initio structures

SCHOLARONE™
Manuscripts

Only

1
2
3
4
5
6
7
8
9
10
11
12 The Solvation of Bromide Anion in Acetonitrile: A
13
14
15
16 Structural Study Based on the Combination of
17
18
19
20 Theoretical Calculations and X-ray Absorption
21
22
23 Spectroscopy
24
25
26

27 Regla Ayala,^a José M. Martínez,^a Rafael R. Pappalardo^a

28
29 Adela Muñoz-Páez^b and Enrique Sánchez Marcos^{a,*}

30
31 (a)Departamento de Química Física and

32
33 (b)Departamento de Química Inorgánica e

34
35 Instituto de Ciencia de Materiales de Sevilla-CSIC

36
37 Universidad de Sevilla. 41012-Sevilla (Spain).

38
39
40
41 e-mail:sanchez@us.es

42
43
44
45 July 24, 2006
46
47
48
49
50
51
52
53
54
55
56
57
58
59
60

Abstract

This work studies the solvation of bromide in acetonitrile by combining quantum mechanics, computer simulations and XANES spectroscopy. Three different sets of interaction potentials were tested, one of them derived from literature and the other two are simple modifications of the previous one to include specificities of the bromide-acetonitrile interactions. Results for microsolvation of bromide were obtained by quantum mechanical optimization and classical minimization of small clusters $[\text{Br}(\text{ACN})_n]^-$ ($n=9,20$). Analysis of MD simulations have provided structural, dynamic and energetic aspects of the solvation phenomenon. The theoretical computation of Br K-edge XANES spectrum in solution using the structural information obtained from the different simulations has allowed the comparison among the three different potentials, as well as the examination of the main structural and dynamic factors determining the shape of the experimental spectrum.

1 INTRODUCTION

Although, halide anions are the most common counter-ions in solution, the investigation of their solvation in aprotic solvents is very limited in comparison with that in water and other protic and polar solvents, such as alcohols.¹ This is in contrast to the increasing importance of this type of solutions due to its technological applications within fields such as separation chemistry, electrochemical devices or ionic recognition.¹⁻³ The non-aqueous solvation structures of halide anions are not completely defined so far owing to both experimental and theoretical difficulties. First of all, the central body of experimental data on halide solvation in non-aqueous solvents does not provide direct structural information. This is usually obtained by using reasonable models compatible with the available data. Spectroscopic and diffraction techniques offer a more direct structural information, but the increase in the number of atom pair contributions to the global distribution function, compared to the water case, renders more difficult the structural elucidation. In addition, the high concentration of the species of interest, usually required by these techniques, does not allow to discard ion-ion contributions from the global signal. For this reason, during the last decade an intense research activity on the study of small clusters has been developed with the aim of separating the ion-solvent from the pure solvent-solvent interactions.^{4,5} On the other hand, theoretical studies of halide solvation are hampered by the fact that the halide-solvent interactions are rather weak leading to a delicate balance between the ion-solvent and solvent-solvent interactions.⁶ This trend becomes particularly significant for bromide and iodide anions and for aprotic and not very polar solvents. Thus, for these two anions, solvation number within the range 1-9 are found in the literature^{2,7,8} when acetonitrile is used as solvent. Furthermore, the structural arrangement adopted by the solvent molecules is far from clear. In this sense, Richardi et al.^{3,8} propose in two theoretical studies based on Molecular Ornstein-Zernike (MOZ) theory, a non-aligned orientation of the solvent molecules with respect to the ion. This is in contrast to the conventional assumption of an ion-dipole interaction dominant according to which the

1
2
3
4
5
6
7 highest stabilization energy would be provided by structures where acetonitrile molecules
8 in contact with the anion would orientate their dipole axis passing through the anion
9 center.
10
11

12
13 Nowadays, X-ray Absorption Spectroscopy (XAS) is a well-established technique to
14 study structural and electronic properties of the local environment of a given atom. A
15 large number of investigations⁹⁻¹¹ have demonstrated the suitability of this technique to
16 study ionic solutions because it requires only short-range order and can be applied to a
17 wide range of concentrations, covering several orders of magnitude (from 10^{-4} M to 10M).¹²
18 The X-ray Absorption spectrum has been traditionally divided into two energy regions.
19 The low energy part of the spectrum, extending up to $\sim 50 - 100$ eV above the absorbing
20 edge, called X-ray Absorption Near Edge Structure (XANES) region and the high energy
21 part of the spectrum (over 100 eV above the threshold up to approximately 1000 eV) called
22 Extended X-ray Absorption Fine Structure (EXAFS). The XANES region has been shown
23 to be dependent on many parameters of the system under study: the oxidation state of
24 the absorber atom, bond angles, coordination geometry, distances of the absorbing atom
25 to the first, and higher coordination shells, etc.¹³ Conversely to the EXAFS region, there
26 is not a simple formulation that encompasses all these parameters. This fact has led to
27 the use of XANES information on a more qualitative level that envisages the spectrum
28 as a “fingerprint” of the system under study. In the last years, implementation of models
29 for the absorption phenomena have allowed the development of codes which accurately
30 simulate the XANES region thus approaching the situation for the EXAFS region.^{14,15} In
31 this way the theoretical simulation of XANES of ionic solutions is an emerging branch.^{16,17}
32
33

34 The aim of this work is to study the bromide solvation structure in acetonitrile by com-
35 bining the experimental information derived from XANES spectroscopy with theoretical
36 data from quantum mechanics calculations and molecular dynamics (MD) simulations.
37 For the latter ones, simple methods to get specific interaction potentials for bromide in
38 acetonitrile are investigated. The interplay of XAS spectroscopy with quantum mechanics
39
40
41
42
43
44
45
46
47
48
49
50
51
52
53
54
55
56
57
58
59
60

1
2
3
4
5
6
7 and numerical simulations has shown to be as an appropriate strategy to get insight into
8 structural information on ionic aqueous solutions,¹⁸⁻²⁷ and will be explored for the case
9 of a non-aqueous solution.
10
11

12
13 In a previous study⁶ dealing with bromide solvation within the framework of a quantum-
14 mechanical approach we showed that the bromide anion interacts with the acetonitrile
15 molecules through the hydrogen atoms of the methyl group. The linear minima are in all
16 cases slightly higher in energy than the bent ones, in good agreement with the findings of
17 Richardi et al.^{3,8} in their statistical simulation of bromide solvation in acetonitrile.
18
19
20
21
22

23
24 In this work, we will use the structural information derived from quantum chemical
25 minimizations and from statistical simulation trajectories using interactions potentials
26 from the literature^{28,29} and simple modification on them (see Section 2.2 for details) to
27 compute the XANES spectra. Direct comparison with the available experimental XANES
28 spectra for this system will allow the definition of new criteria to examine the validity of
29 the results and conclusions reached, as well as to explore an additional way to define and
30 validate intermolecular potentials.
31
32
33
34
35
36
37
38
39

40 2 COMPUTATIONAL METHODS.

41
42
43 . The analysis of the structural results derived from computations is based on the ex-
44 amination of the main features of the simulated XANES spectra and their comparison
45 with the experimental one. An input structure, as detailed as possible, is required since
46 XANES is particularly sensitive to the close environment. The source of structures to
47 be used for the simulated spectra have a double origin. First, clusters formed by one
48 bromide anion and an increasing number of acetonitriles molecules computed at quantum
49 mechanical level. Second, snapshots extracted from the molecular dynamics trajectories
50 of a bromide anion immersed in a large number of acetonitrile molecules simulating the
51 solution, at room temperature. The computer simulations have not been limited to apply
52 combination rules to obtain the appropriate intermolecular potentials from the literature,
53
54
55
56
57
58
59
60

1
2
3
4
5
6
7 but some easy to implement procedures have been applied to obtain new potentials. Their
8 validity is discussed by checking the simulation results in the light of the XANES spectrum
9 and other available experimental data.
10
11
12

13 14 15 **2.1 Quantum Mechanical Computations**

16
17 The starting structures were taken from a previous work⁶ dealing with the microsolvation
18 of the bromide anion in water, methanol and acetonitrile. The bromide-acetonitrile
19 cluster were optimized at B3LYP level with the 6-31+G* basis set. The energy mini-
20 mized $[\text{Br}(\text{ACN})_9]^-$ structure was characterized as minimum in the PES of the bromide-
21 acetonitrile system. Gaussian03 suite of programs were used for computations.³⁰
22
23
24
25
26
27
28
29

30 **2.2 Molecular Dynamics Simulations.**

31
32 Three different sets of interaction potentials have been used to simulate the solvation of
33 bromide anion in acetonitrile at room temperature (298K):
34
35

- 36
37 • The first set was built from the recent model of Grabuleda et al.²⁸ for acetonitrile
38 liquid, whereas bromide anion was described by the parametrization performed by
39 McCammon and col.²⁹ In both cases, potential parameters were developed in the
40 framework of the Cornell et al.³¹ force field providing flexible all-atom models for
41 the acetonitrile molecules. Internal deformations were allowed by means of the
42 usual bond, angle, and torsion terms, while the non-bonded van der Waals and
43 electrostatic terms were used to describe the intermolecular interactions. This set
44 of potentials will be labeled Pot-A (in this set of potentials, the combination rule
45 leads to a value for the van der Waals parameter of the Br-H pair $\sigma_{\text{Br-H}}=3.6 \text{ \AA}$).
46
47
48
49
50
51
52
53
54
55
56
- 57 • The second set of potentials tested was a simple modification of the previous one,
58 based on the hydrated ion concept developed by our group for the cation hydration
59 case.³² The solvated bromide cluster with $n=9$, $[\text{Br}(\text{ACN})_9]^-$, was used as a reference
60

1
2
3
4
5
6
7 structure to modify the van der Waals parameter $\sigma_{\text{Br-H}}$. For this purpose, that
8 parameter was chosen in such a way that the atomic root mean square deviation
9 (RMSD) between the quantum mechanical and force field optimized structure was
10 minimized. The optimum value was $\sigma_{\text{Br-H}} = 3.2 \text{ \AA}$ (RMSD=0.7 \AA , the superposition
11 of both structures is shown in Figure 1). This set of potentials will be labeled Pot-B.
12
13
14
15
16

- 17
18 • In a similar way, a third set of potentials was used by modifying the $\sigma_{\text{Br-H}}$ parameter
19 in order to test the sensitivity of the Br K-edge XANES spectrum of bromide in
20 acetonitrile to changes in the closest environment of the absorber atom, as well as
21 to other properties of the solution. Bearing in mind that the value of this parameter
22 in the first set of interaction potentials was 3.6 \AA , and 3.2 \AA for the second set, a
23 value of 2.9 \AA for $\sigma_{\text{Br-H}}$ was chosen. Thus, a range of 0.7 \AA [2.9-3.6] will be used
24 to get insight into the relationships between spectrum and structure, on one hand,
25 and between solution properties and σ values, on the other. This set of potentials
26 will be labeled Pot-C.
27
28
29
30
31
32
33
34
35
36

37 The elementary simulation cell contained 1 bromide ion and 500 acetonitrile molecules.
38 The length of the cubic cell, $L = 30.30 \text{ \AA}$, was set to reproduce the experimental value for
39 the density of liquid acetonitrile at 25 $^{\circ}\text{C}$. Periodic boundary conditions were applied. A
40 time step of 0.25 fs was used. The cut-off distance for the non-bonding interactions was
41 $L/2 \text{ \AA}$. Long-range interactions were incorporated by means of Ewald summation.³³ The
42 system was equilibrated at the chosen temperature for 50 ps, and 500 ps of simulation time
43 was produced in the *NVT* ensemble for each set of the interaction potentials considered.
44 The average temperature was maintained constant at 300K by a Berendsen thermostat³⁴
45 with a time constant of 0.5 ps. Structures were saved every 2 ps for further analysis.
46 The MD simulations were performed with DLPOLY program,³⁵ running on a parallel
47 multiprocessor SGI ALTIX 350 computer using 20 processors.
48
49
50
51
52
53
54
55
56
57
58
59
60

2.3 Computation of XANES spectra.

The K-edge XANES spectrum of bromide in acetonitrile was computed for several structures. On one hand, cluster optimized structures involving 9 acetonitrile molecules ($[\text{Br}(\text{ACN})_9]^-$) were performed, the origin of the structures being quantum mechanically or potential derived, as well as for a $[\text{Br}(\text{ACN})_{20}]^-$ cluster optimized with the set of intermolecular potentials Pot-B. On the other hand, XANES spectra obtained from MD trajectories employing 100 snapshots equally spaced (taken every 5 ps) were also produced for all the interaction potential sets. The final simulated XANES spectrum from the MD simulation correspond to the averages over the spectra of each snapshot set.

The FEFF8.10 code program developed by Rehr's group was used to calculate the spectra.¹⁵ The potential calculations use the Hedin-Lundqvist self-energy approximation.³⁶ A self-consistent field procedure (SCF) was employed. A 6.0 Å cutoff radius was chosen for the SCF treatment and for the full-multiple scattering paths. A full-multiple scattering path calculation was done taking as origin the absorber atom, i.e. the bromide anion. Then, the chosen structure included the backscatter atoms inside a sphere of 6.0 Å radius centered at the bromide. However, for the SCF procedure, for each type of atom the origin of the cutoff radius was placed in that atom, what means that the region of the solution considered for calculation is increased by the distance between the bromide anion and the corresponding atom. This SCF procedure introduces a difference between the XANES computation derived from quantum mechanical or statistical calculations, as the size of the solvent sphere surrounding the anion is, in general, not complete for all the types of atoms when clusters optimized quantum-mechanically are considered. A XANES spectrum calculated from 250 snapshots taken every 2 ps configurations yields very similar results to the one obtained using 100 snapshots taken every 5 ps. The consideration of a larger cutoff radius, such as 7.0 Å in the SCF computation of the wavefunction to determine potentials and/or XANES spectra calculation do not affect the results.

In a previous work²⁷ on bromide hydration structure, it was necessary to include the

1
2
3
4
5
6
7 hydrogen atoms to obtain a realistic backscattering potential and a simulated XANES
8 spectrum that resembled experimental data. This could be understood by the fact that
9 hydrogen atoms form the closer shell around the anion. The bromide ion induces the
10 presence of a set of hydrogen atoms of first-shell water molecules in its closest vicinity,
11 which are found to play a significant role in both the scattering phenomenon and in the
12 determination of electronic wavefunctions of the bromide clusters. For the same reason,
13 hydrogen atoms were included in the calculation of both backscattering potential and
14 XANES spectrum in this work.
15
16
17
18
19
20
21
22
23
24

25 **3 RESULTS AND DISCUSSION.**

26 **3.1 MD analysis.**

27
28
29
30
31
32 Results of the MD analysis are summarized in Figure 2, where the Br-H and Br-C(methyl)
33 radial distribution functions (RDFs) are plotted, and in Table 1, where a set of structural
34 parameters, solvation energy and translational self-diffusion coefficient for the bromide
35 anion are collected. The Br-H RDF exhibits a double peak for the first solvation shell
36 which indicates that the three hydrogen atoms of the methyl group are not symmetrically
37 distributed around the bromide anion. The running coordination number gives a ratio 1:2
38 between the two peaks, and the total number of atoms up to the second minimum (5.5-5.9
39 Å in Figure 2a) is around 30-33 atoms, depending on the potential set employed. These
40 RDFs reflect the different value of the $\sigma_{\text{Br-H}}$ parameter employed. The maximum of the
41 first peak appears at 3.28 Å for Pot-A ($\sigma_{\text{Br-H}}= 3.6$ Å), at 2.93 Å for Pot-B ($\sigma_{\text{Br-H}}=3.2$ Å)
42 and at 2.73 Å for Pot-C ($\sigma_{\text{Br-H}}=2.9$ Å). The mean angle BrHC (α) collected in Table 1
43 for the closest hydrogen atom to the anion is also reflecting the increasing directionality
44 of the hydrogen bond (a strong hydrogen bonding is roughly linear, i.e. an angle value
45 for XHY close to 180°): 125° for Pot-A, 135° for Pot-B and 145° for Pot-C. The asym-
46 metrical solvation of the methyl group implies that the charge(anion)-dipole(acetonitrile)
47
48
49
50
51
52
53
54
55
56
57
58
59
60

1
2
3
4
5
6
7 interaction is not the dominant contribution in the first solvation shell. Angle β defines
8 the angle formed by the molecular axis of the acetonitrile molecule and the vector formed
9 by the bromide and the center of mass of the acetonitrile molecule (Scheme 1). A β value
10 equals to 0° indicates the alignment of the anion with the molecular axis. Table 1 shows
11 that the average β value is in the range $66\text{-}80^\circ$, then the structural arrangement for the
12 first solvation agrees with the results obtained by Richardi et al.^{3,8} from MOZ theory and
13 MC simulations.
14
15
16
17
18
19
20

21 Br-C(methyl) RDFs for the three potentials are presented in Figure 2b. The maximum
22 of the first peak is found in the range $3.7\text{-}4.0\text{\AA}$, running integration numbers correspond
23 roughly to 10 acetonitrile molecules. The height and width of the peaks for the three
24 potentials show that the smaller $\sigma_{\text{Br-H}}$ is, the more compact the first solvation shell is.
25 Experimental estimations of coordination numbers around bromide vary in a wide range,
26 from dielectric relaxation measurements and thermodynamic data a value of 2 is ob-
27 tained,^{2,7} whereas from EXAFS measurements the value is close to 5.³⁷ This EXAFS
28 study also gives a Br-C distance of 3.48 \AA which has associated a large Debye-Waller
29 factor, $\sigma^2 = (\overline{R_{\text{Br-C}} - R_{\text{Br-C}}})^2 = 0.162\text{ \AA}^2$, implying a large static and dynamic disorder asso-
30 ciated to the Br-C parameter. When comparing these DW factors with those computed
31 from MD simulations (see Table 1), estimations are larger than the experimental one,
32 when using Pot-A a value of 0.28 \AA^2 is obtained, whereas Pot-B and Pot-C give a similar
33 and smaller value of 0.21 \AA^2 . EXAFS equation presents a strong coupling between the co-
34 ordination number and the associated DW factors, whereas the first parameter contributes
35 to increase the intensity of the signal (the larger the number of backscatter atoms, the
36 more intense the signal becomes), the second parameter contributes to damp the inten-
37 sity of the signal (the larger the static and dynamic disorder around the absorber atom
38 are, less intense the signal is). Thus, for a given intensity, small values of DW factors are
39 compatible with small coordination numbers, as well as larger DW factors will need larger
40 coordination numbers. The theoretical trend of the DW factors reflects that lowering the
41
42
43
44
45
46
47
48
49
50
51
52
53
54
55
56
57
58
59
60

1
2
3
4
5
6
7 $\sigma_{\text{Br-H}}$ parameter reinforces the bromide-acetonitrile interactions with respect to the MD
8 simulation with Pot-A, giving rise to tighter structures, although they are more relaxed
9 than the experimental one.
10
11

12
13 Regarding coordination number, Richardi et al.⁸ from their molecular Ornstein-
14 Zernike (MOZ) study predicts a value close to 9.5 molecules of acetonitrile in the first
15 solvation shell. In a later work, these authors carry out a study of halides in acetonitrile,
16 excluding bromide, comparing MOZ and MonteCarlo simulations.³ Maxima for the first
17 shell of X-C (X \equiv Cl and I) RDFs appear at ca. 3.8 and 4.3 Å for chloride and iodide
18 respectively, what may represent a reasonable range to enclose the Br-C distance.
19
20
21
22
23
24

25 The experimentally estimated enthalpy of solvation² is -337 kJ/mol, whereas the com-
26 puted value for the three simulations ranged between -260 and -285 kJ/mol. The sequence
27 of solvation energies for the three set of potentials follows the same order than the value of
28 $\sigma_{\text{Br-H}}$ and the corresponding distance of the first shell of acetonitrile around the halide.
29 Richardi et al.⁸ obtain similar results from their simulation when the Gibbs solvation free
30 energy are estimated, the theoretical values underestimate (provide less negative values)
31 the experimental data in 30-60 kJ/mol.
32
33
34
35
36
37
38
39

40 The translational self-diffusion coefficient for the bromide has been computed from
41 the mean-square displacement function by following the Einstein relation, theoretical D_{Br}
42 values are found to be in the range $1.4\text{-}1.6\cdot 10^{-9}$ m²s⁻¹. There is no previous theoretical
43 estimation for D_{Br} in acetonitrile, but Guardià and Pinzon³⁸ have computed D_{Cl} from MD
44 simulations of chloride in acetonitrile, finding a value of $1.8\cdot 10^{-9}$ m²s⁻¹. The experimental
45 values derived from conductivity measurements are 2.66 and $2.67\cdot 10^{-9}$ m²s⁻¹ for chloride
46 and bromide, respectively.³⁹
47
48
49
50
51
52
53
54
55

56 **3.2 XANES spectra from $\text{Br}(\text{ACN})_n^-$ clusters**

57

58 The usual way to relate geometrical structure around an absorber atom in a solid and fea-
59 tures of XANES spectra is by means of the simulation of the spectrum from a reasonable
60

1
2
3
4
5
6
7 geometry generally taken from crystallographic data or some related structural model.
8
9 Nevertheless, when one deals with a structure in solution the source of structural infor-
10 mation is scarce. An strategy to get advantages of both the experimental and theoretical
11 sources of information is to simulate spectra from the structure provided by theoretical
12 methods and to compare them with the experimental spectra. A synergy may be estab-
13 lished, such that theoretical procedures could be improved by approaching the computed
14 spectrum to the experimental one, and simultaneously the structural information derived
15 from the spectrum is refined, and the features of the spectra properly assigned.
16
17
18
19
20
21
22

23 First of all, we are going to compare the XANES spectra obtained for clusters formed
24 by one bromide anion and a number of acetonitrile molecules small enough to define only
25 the first solvation shell $[\text{Br}(\text{ACN})_9]^-$, subsequently, the first and second solvation shells will
26 be included, $[\text{Br}(\text{ACN})_{20}]^-$, and both spectra compared. Figure 3 includes comparative
27 plots of the experimental spectrum obtained by Watanabe and col.³⁷ with those computed
28 for the optimized structures $[\text{Br}(\text{ACN})_9]^-$ obtained by applying the three sets of potentials
29 and the quantum mechanical level. The spectra obtained from the structures derived
30 quantum mechanically by using Pot-B and Pot-C present the three main resonances and
31 their relative intensities are quite similar to the experimental spectrum. On the contrary,
32 Pot-A derived structure leads to a quite different ratio of intensities which makes the
33 computed spectrum rather different in shape from the experimental one, even though
34 resonances appears at the same energy values. The spectrum derived from the structure
35 optimized quantum-mechanically has been over-imposed to that derived of Pot-B to show
36 the sensitivity of XANES features to small changes, since the fitted $\sigma_{\text{Br-H}}$ value was
37 chosen just to bring the potential-derived structure containing nine acetonitrile molecules
38 as close as possible to quantum-mechanical one. (The RMS for the structure was 0.7 Å,
39 and Figure 1 shows the similarity between both structures). The changes that a second
40 solvation shell induces on the spectrum features can be observed in the XANES generated
41 for the $[\text{Br}(\text{ACN})_{20}]^-$ cluster (obtained through the use of Pot-B). The comparison with
42
43
44
45
46
47
48
49
50
51
52
53
54
55
56
57
58
59
60

1
2
3
4
5
6
7 the nona-acetonitrilated cluster for Pot-B suggests that second-shell effects are marginal:
8
9 a small change in the relative intensities of the three resonances and a slight smoothing,
10
11 both at the white line and at the high-energy part of the spectrum. It is worth noting
12
13 that the computed spectra show more intense features at the high energy region than the
14
15 experimental one. This is a consequence of the rigidity and symmetry of the structures
16
17 used, since their origin is an energy minimization. In contrast, the spectrum obtained for a
18
19 cluster of 20 acetonitrile molecules but whose structure is a snapshot of the MD trajectory
20
21 with Pot-B is smeared out and the intensity of the second resonance is reduced.
22

23
24 To show the relationships between XANES features and structure around bromide,
25
26 Figure 4 plots the distribution of the distances for the two first types of backscatter atoms
27
28 surrounding the halide, that is hydrogen and carbon atoms of acetonitrile molecules.
29
30 Ordinate contains the corresponding distance of the backscatter atoms to the bromide
31
32 whereas abscissa gives the order number established on the basis of the H(or C)-Br dis-
33
34 tance. Thus, the curve $R_{\text{Br-H}}$ vs. n_H for the minimum $[\text{Br}(\text{ACN})_9]^-$ structure obtained
35
36 quantum-mechanically shows nine H atoms placed at 2.79-2.90 Å. The additional 18 hy-
37
38 drogen atoms of the cluster are placed at larger distances within the range 4.30-4.60Å.
39
40 The structure obtained by Pot-A exhibits the most distant first shell of H atoms, located
41
42 in between the two previous ranges of distances (3.2-3.5 Å) and with almost a double
43
44 number of backscatters (15). Its XANES spectrum is that differing most from the exper-
45
46 imental one. An intermediate distribution is shown by the snapshot with 20 molecules,
47
48 where $R_{\text{Br-H}}$ values increases monotonically, although the closest distances are more sim-
49
50 ilar to the two minimum geometries obtained with Pot-B. In the case of the optimized
51
52 cluster with 20 solvent molecules using the set of potentials B, the shape of the spectrum
53
54 is more similar to the corresponding structure with 9, indicating that the second set of
55
56 H atoms play a minor role on the XANES features. It is worth pointing out that the
57
58 sequence of Br-H distance for Pot-C, Pot-B and quantum mechanics compared with the
59
60 energy gap between the two first resonances illustrates pretty well the Natoli's rule,¹³

1
2
3
4
5
6
7 i.e. the difference in energy between the white line and the energy of a given feature is
8
9 inversely proportional to the coordination distance of the shell of atoms related with this
10
11 feature. The Br-C distributions show a sequence of distances for the first shell of atoms
12
13 which differs from that obtained for the Br-H one. Thus, the quantum mechanical cluster
14
15 bears the longest $R_{\text{Br-C}}$ for the seven closest C atoms to Br. This is a consequence of
16
17 the less twisted orientation of the acetonitrile molecules around the bromide anion, i.e.
18
19 a smaller value of the α angle (See Scheme 1 and Figure 1). The $[\text{Br}(\text{ACN})_9]^-$ clusters
20
21 for Pot-B, Pot-C and quantum mechanics level, as well as the $[\text{Br}(\text{ACN})_{20}]^-$ for Pot-B
22
23 retains similar shape of $R_{\text{Br-C}}$ distributions than the R_{BrH} ones. There is a plateau of
24
25 $R_{\text{Br-C}}$ for the first shell of C atoms which denotes the consistency of the shell in these
26
27 simulations. In fact this pattern, which is defined by a regular coordination sphere of C
28
29 atoms placed at quite similar distance of bromide, seems to be the most direct contri-
30
31 bution to the XANES features. In particular, the intensity of the second resonance and
32
33 the relative height of the white line with respect to the second resonance are affected by
34
35 the $R_{\text{Br-C}}$ value and the symmetry of its distribution. This is observed when the XANES
36
37 spectrum is computed for two modified structures of the quantum mechanic $[\text{Br}(\text{ACN})_9]^-$
38
39 minimum, where selectively the Br-C distance is changed by +0.1 and -0.1 Å.
40
41

42 As previously remarked in the literature,^{16,25,26,40} these findings show that for the
43
44 XANES definition is essential the geometrical arrangement of atoms around the photo-
45
46 absorber, such that slightly different structures could lead to clearly different spectra.
47
48
49

50 3.3 XANES spectra from MD simulations.

51
52 The computed Br K-edge XANES spectrum of bromide in acetonitrile solution at 298K
53
54 obtained from MD simulations which used the three different set of potentials are shown
55
56 in Figure 5. In contrast with the structure of clusters, these spectra are the average
57
58 for a large number of structures (100 snapshots) which result from the fluctuations of
59
60 the solvent structure around the bromide. The relevance of the changes induced by

1
2
3
4
5
6
7 the fluctuation might be seen either by individual inspection of spectra corresponding
8 to several snapshots or by drawing the standard deviation of the absorption line along
9 the whole energy range. These two plots have been included in Figure 6. The individual
10 XANES spectra coming from different snapshots show significant differences among them,
11 specially at low energy. The interesting fact derived from this figure is that the majority
12 of the individual spectra are quite different to the average. This stresses the importance
13 of carrying out a thorough sampling of the configurational space to properly compute the
14 XANES spectra in solution. This is not surprising if one bears in mind the differences
15 originated in the XANES features when using the different clusters studied in the previous
16 section. Similar results were found in an earlier theoretical-experimental study on the
17 hydration of bromide.²⁷ Geometrical fluctuations generates quite different local hydration
18 environments around bromide, then leading to quite different shape of spectra derived by
19 each individual snapshot (for instance see Figure 2 in ref [27]).
20
21
22
23
24
25
26
27
28
29
30
31
32

33 As shown in Figure 5, the spectrum computed from the MD snapshots of Pot-A gives
34 a rather poor reproduction of the experimental spectrum, something that was already ob-
35 served for the minimized structure using this potential (Figure 3). The other two spectra
36 are more similar to the experimental one, although in both cases the relative intensity of
37 the second resonance decreases with respect to the simulated XANES obtained with their
38 corresponding optimized clusters (Figure 3). On the contrary, the global shape of these
39 spectra are smoother compared to the non-statistically averaged spectra obtained for the
40 clusters. Thus, the tail of the XANES is smeared out in contrast to the XANES computed
41 for clusters and the global spectrum is damped by the statistical average. Considering the
42 magnitude of the deviations of the individual spectra with respect to the averaged one,
43 it could be surprising the similarity among the experimental spectra and those obtained
44 from the cluster structures (quantum mechanics or classical potentials, Pot-B and Pot-
45 C), which are based on an unique structure, that of the minimum for each cluster size.
46 Nevertheless, there is a fundamental difference between the snapshots and the structures
47
48
49
50
51
52
53
54
55
56
57
58
59
60

1
2
3
4
5
6
7 derived of an energy minimization. The latter ones are the direct consequence of the bal-
8
9 anced interaction potentials operating in the system (represented by a cluster of a given
10
11 size) and, on this basis they could be considered as single representative configurations.
12
13 When solvation of a monoatomic ion is considered, a relatively small region of the solvent
14
15 around the ion is perturbed by it, so that the microscopic picture could be envisaged as
16
17 that of an ionic cluster immersed in a pure solvent. The short-range sensitivity of the
18
19 XANES spectroscopy implies that a cluster of a few angströms around the ion is respon-
20
21 sible of the spectrum shape. When the ion-solvent interactions are stronger than the
22
23 solvent-solvent ones, the fluctuations of the solvent molecules in the closer environment
24
25 of the ion (and simultaneously the absorber atom) are small and an averaged structure
26
27 may be representative of the ion solvation shells. Even more, strong attractive interac-
28
29 tions around the ion promotes a quite harmonic behavior of the ion-solvent interactions in
30
31 this region which generates averaged structures quite consistent with those corresponding
32
33 to the potential energy minimizations. The comparison of experimental and computed
34
35 XANES indicates that the main features of the spectrum are pretty well reproduced by
36
37 some of the energy optimized clusters, that is, these structures are representative ones,
38
39 although the fluctuations included by the averaging of snapshots is needed to smear out
40
41 the whole spectrum.
42

43
44 When comparing the distribution of distances for the first backscatters of bromide
45
46 in the clusters (Figure 3) and the peak of the corresponding RDF in Figure 2, a shift
47
48 appears in the Br-H distance of about 0.15 Å from the optimized clusters Pot-B and Pot-
49
50 C to their first maxima in Br-H RDF, in addition to wide peaks that allows a significant
51
52 range of asymmetric arrangements compatible with the dynamic of the system. This
53
54 shifting indicates that solvent effects and/or temperature effects induces a significant
55
56 relaxation of the first solvation shell for the set of potentials Pot-B and Pot-C, where the
57
58 bromide-acetonitrile interactions may become stronger in the first shell. Since the main
59
60 parameter changing with $\sigma_{\text{Br-H}}$ is just the Br-H distance, when going from structures of

1
2
3
4
5
6
7 minimum for clusters in gas phase to solution, the interactions between the solvated ion
8 and bulk solvent and those between the solvent-solvent molecules play a role equivalent
9 to an increase of this parameter. The maxima of g_{Br-H} is 2.73 and 2.93 Å for Pot-C and
10 Pot-B, respectively (see Table 1 and Figure 2) whereas in the corresponding $[Br(ACN)_9]^-$
11 clusters are around 2.55 and 2.75 Å. The solvent effects on the Br-C distances are much
12 smaller in these two simulations, which indicates a decrease of the orientational angles α
13 and β (See Scheme 1). This is one of the reasons that makes the computed XANES more
14 similar to the experimental one is that derived from MD simulation with Pot-C.
15
16
17
18
19
20
21
22

23 It is interesting to notice that previous studies on cation hydration²⁴⁻²⁶ following the
24 same methodology have shown that the mismatch between individual spectra and the
25 averaged one is less important than that observed in the anion solvation.²⁷ The reason is
26 that anion-solvent interactions are weaker than the cation-solvent ones. Additional factors
27 derived from simulation contribute to modify the shape of the spectrum whose detailed
28 analysis can not be easily split. A general conclusion is that for the set of potentials em-
29 ployed, the acetonitrile-acetonitrile interactions are too much dominant with respect to the
30 bromide-acetonitrile ones. Provided that acetonitrile simulations of the pure solvent gives
31 consistent results,²⁸ a strategy to improve the description of the bromide solution could be
32 to define a more attractive bromide-acetonitrile interaction potential by including in the
33 fitting ab initio interaction energies of clusters, in addition to geometrical criteria. Like-
34 wise, as pointed out by Richardi et al.³ for the case of aprotic solvents, or by Ayala et al.⁴¹
35 for the case of water, the consideration of a polarizable model certainly must introduce
36 some improvements in the detailed balance among the ion-solvent and solvent-solvent in-
37 teractions. The results derived from simulations are consistent with previous simulations
38 of related systems, using other intermolecular potentials and/or computational modeling,
39 such as integral equations or Monte Carlo.¹
40
41
42
43
44
45
46
47
48
49
50
51
52
53
54
55
56
57
58
59
60

4 Concluding Remarks.

Simulations of bromide in acetonitrile have been carried out by means of the use of interaction potentials available in the literature, and simple modifications of them based on structural criteria associated to the hydrated ion concept.

The structural description of the local environment of bromide anion in acetonitrile is a rather relaxed first solvation shell formed by ca. 10 acetonitrile molecules where one of the hydrogen atoms of the methyl group is placed closer to the anion, 2.7-2.9 Å, than the other two hydrogen atoms of the methyl group (ca. 4.2-4.4 Å) due to the bent orientation of the acetonitrile molecules (aprox. 130 °) with respect to the bromide anion. This allows the carbon atom of the methyl group to be closer to the bromide, ca. 3.7-3.8 Å. A small second peak at 8 Å shows a quite diffuse shell that is more dominated by the acetonitrile solvent structure than by the anion.

Taken into account that different theoretical approaches have been employed as source of structural information, several solvation environment around the bromide have been described, allowing us a detailed analysis of the relationship between structures, XANES features and static and dynamic disorder of the solution. Given the difficulty of establishing a direct relation with other observables in solution, XANES (and EXAFS) has revealed as an interesting guide to validate or improve computer simulations. In this particular case, it has been shown that the coordination shells beyond the first one do not make an important contribution to the spectrum.

The resemblance between the theoretical spectra obtained from quantum mechanically optimized clusters ($n \geq 9$) and the average spectra derived from MD simulations with some of the set of potentials allows us to conclude that those clusters are a good model picture of the structure of bromide in acetonitrile. Nonetheless, the discrepancies among the individual spectra derived from MD simulations indicate that this representation should be taken as an average model picture with important standard deviations. The set of potential called Pot-B seems the most appropriate to deal with small clusters of

1
2
3
4
5
6
7 [Br(ACN)_n]⁻ (for n ≥ 20), whereas the set Pot-C seems the more convenient to describe
8
9 acetonitrile solutions containing bromide.
10

11 12 13 **5 Acknowledgments** 14

15
16 This work was supported by Spanish DGICYT (CTQ2005-03657).
17
18
19
20
21
22
23
24
25
26
27
28
29
30
31
32
33
34
35
36
37
38
39
40
41
42
43
44
45
46
47
48
49
50
51
52
53
54
55
56
57
58
59
60

References

1. Barthel, J. M. G.; Krienke, H.; Kunz, W. *Physical Chemistry of Electrolyte Solutions*; Steinkopff: Darmstadt, 1998.
2. Marcus, Y. *Ion Solvation*; Wiley: Chichester, 1985.
3. Fischer, R.; Richardi, J.; Fries, P. H.; Krienke, H. *J. Chem. Phys.* **2002**, *117*, 8467.
4. Markovich, G.; Cheshnovsky, O.; Perera, L.; Berkowitz, M. L. *J. Chem. Phys.* **1996**, *105*, 2675.
5. Megyes, T.; Radnai, T.; Wakisaka, A. *J. Mol. Liq.* **2003**, *103-104*, 319.
6. Ayala, R.; Martínez, J. M.; Pappalardo, R. R.; Sánchez Marcos, E. *J. Phys. Chem. A* **2000**, *104*, 2799.
7. Barthel, J.; Kleebauer, M.; Buchner, R. *J. Solution Chem.* **1995**, *24*, 1.
8. Richardi, J.; Fries, P. H.; Krienke, H. *J. Chem. Phys.* **1998**, *108*, 4079.
9. Koningsberger, D. C.; Prins, R., Eds.; *X-Ray Absorption: Principles, Applications, Techniques of EXAFS, SEXAFS, and XANES*; Wiley: New York, 1988.
10. Ohtaki, H.; Radnai, T. *Chem. Rev.* **1993**, *93*, 1157.
11. Richens, D. T. *The Chemistry of Aqua Ions*; John Wiley: Chichester, 1997.
12. Muñoz-Páez, A.; Pappalardo, R.; Sánchez Marcos, E. *J. Am. Chem. Soc.* **1995**, *117*, 11710.
13. A. Bianconi, X-Ray Absorption: Principles, Applications, Techniques of EXAFS, SEXAFS and XANES. In ; Koningsberger, D. C.; Prins, R., Eds.; John Wiley: New York, 1988.

- 1
2
3
4
5
6
7 14. Natoli, C. R.; Benfatto, M.; Brouder, C.; Ruiz López, M. F.; Foulis, D. L. *Phys.*
8 *Rev. B* **1990**, *42*, 1944.
9
10
11 15. Ankudinov, A.; Ravel, B.; Rehr, J. J.; Conradson, S. D. *Phys. Rev. B* **1998**, *58*,
12 7565.
13
14
15 16. Benfatto, M.; Solera, J. A.; Chaboy, J.; Proietti, M. G.; García, J. *Phys. Rev. B*
17 **1997**, *56*, 2447.
18
19
20 21. Díaz-Moreno, S.; Muñoz-Páez, A.; Chaboy, J. *J. Phys. Chem. A* **2000**, *104*, 1278.
22
23
24 25. Palmer, B. J.; Pfund, D. M.; Fulton, J. L. *J. Phys. Chem.* **1996**, *100*, 13393.
26
27
28 29. Roccatano, D.; Berendsen, H. J. C.; D'Angelo, P. *J. Chem. Phys.* **1998**, *108*, 9487
29 and references therein.
30
31
32 33. Filipponi, A.; D'Angelo, P.; Pavel, N. V.; Di Cicco, A. *Chem. Phys. Lett.* **1994**,
34 225, 150.
35
36
37 38. Spångberg, D.; Hermansson, K.; Lindqvist-Reis, P.; Jalilehvand, F.; Sandström, M.;
39 Persson, I. *J. Phys. Chem. B* **2000**, *104*, 10467.
40
41
42 43. Jalilehvand, F.; Spångberg, D.; Lindqvist-Reis, P.; Hermansson, K.; Persson, I.;
44 Sandström, M. *J. Am. Chem. Soc.* **2001**, *123*, 431.
45
46
47 48. Campbell, L.; Rehr, J. J.; Schenter, G. K.; McCarthy, M. I.; Dixon, D. *J. Syn-*
49 *chrotron Radiat.* **1999**, *6*, 310.
50
51
52 53. Merklings, P. J.; Muñoz-Páez, A.; Martínez, J. M.; Pappalardo, R. R.; Sánchez
54 Marcos, E. *Phys. Rev. B* **2001**, *64*, 012201.
55
56
57 58. Merklings, P. J.; Muñoz-Páez, A.; Pappalardo, R. R.; Sánchez Marcos, E. *Phys. Rev.*
59 *B* **2001**, *64*, 092201.
60

- 1
2
3
4
5
6
7 26. Merklings, P. J.; Muñoz-Páez, A.; Sánchez Marcos, E. *J. Am. Chem. Soc.* **2002**, *124*,
8 10911.
9
10
11 27. Merklings, P. J.; Ayala, R.; Martínez, J.; Pappalardo, R.; Sanchez Marcos, E. *J.*
12 *Chem. Phys.* **2003**, *119*, 6647.
13
14
15 28. Grabuleda, X.; Jaime, C.; Kollman, P. A. *J. Comput. Chem.* **2000**, *21*, 901.
16
17
18 29. Lybrand, T. P.; Ghosh, I.; McCammon, J. A. *J. Am. Chem. Soc.* **1985**, *107*, 7793.
19
20
21 30. Frisch, M. J.; Trucks, G. W.; Schlegel, H. B.; G. E. Scuseria, M. A. R.; et. al.,
22 *Gaussian 03*; Gaussian, Inc.: Wallingford CT, 2004.
23
24
25 31. Cornell, W. D.; Cieplak, P.; Bayly, C. I.; Gould, I. R.; Merz, K. M.; Fergus-
26 son, D. M.; Spellmeyer, D. C.; Fox, T.; Caldwell, J. W.; Kollman, P. A. *J. Am.*
27 *Chem. Soc.* **1995**, *117*, 5179.
28
29
30 32. Martínez, J.; Pappalardo, R. R.; Sánchez Marcos, E. *J. Am. Chem. Soc.* **1999**, *121*,
31 3175.
32
33
34 33. Allen, M. P.; Tildesley, D. J. *Computer Simulation of Liquids*; Oxford University
35 Press: Oxford, 1987.
36
37
38 34. Berendsen, H.; Postma, J.; van Gusteren, W.; DiNola, A.; Haak, J. *J. Chem. Phys.*
39 **1984**, *81*, 3684.
40
41
42 35. Smith, W.; Forester, T. R. "DL_POLY 2.13", 1996.
43
44
45 36. Hedin, L.; Lundqvist, S. *Solid State Phys.* **1969**, *23*, 1.
46
47
48 37. Sawa, Y.; Miyanaga, T.; Tanida, H.; Watanabe, I. *J. Chem. Faraday Trans.* **1995**,
49 *91*, 4389.
50
51
52 38. Guardià, E.; Pinzón, R. *J. Mol. Liquids* **2000**, *85*, 33.
53
54
55
56
57
58
59
60

- 1
2
3
4
5
6
7 39. Krumgalz, B. S. *J. Chem. Soc. Faraday Trans. 1* **1983**, 79, 571.
8
9
10 40. D'Angelo, P.; Benfatto, M.; Della Longa, S.; Pavel, N. V. *Phys. Rev. B* **2002**, 66,
11 0642091.
12
13
14 41. Ayala, R.; Martínez, J.; Pappalardo, R.; Saint-Martin, H.; Ortega-Blake, I.;
15 Sánchez Marcos, E. *J. Chem. Phys.* **2002**, 117, 10512.
16
17
18
19
20
21
22
23
24
25
26
27
28
29
30
31
32
33
34
35
36
37
38
39
40
41
42
43
44
45
46
47
48
49
50
51
52
53
54
55
56
57
58
59
60

Table 1. MD Results

Potentials	Structural Results				
	$R_{max}(g_{Br-H})(\text{\AA})$	$R_{max}(g_{Br-C(methyl)})(\text{\AA})$	$\sigma_{Br-C}^2 (\text{\AA}^2)$	$\bar{\alpha} (\text{\textcircled{C}})$	$\bar{\beta} (\text{\textcircled{C}})$
A	3.28	4.01	0.28	125	66
B	2.93	3.78	0.21	135	77
C	2.73	3.68	0.21	145	80
	$E_{solv}(\text{kJ mol}^{-1})$		D ($10^{-9} \text{ m}^2 \text{ s}^{-1}$)		
A	-259.2.		1.6±0.1		
B	-275.9		1.6±0.1		
A	-284.5		1.4±0.1		

Figure legends.

Figure 1. Quantum Mechanically optimized structure (blue) for $[\text{Br}(\text{ACN})_9]^-$ cluster together with the minimum RMSD configuration (yellow) according to the $\sigma_{\text{Br}-\text{H}}$ parameter (see text for details).

Figure 2. Radial distribution functions for Br-H and Br-C(methyl) pairs of pot.A, pot.B and pot.C simulations.

Figure 3. Experimental Br K-edge XANES spectrum (black) and theoretically simulated spectra for different bromide-acetonitrile clusters.

Figure 4. Br-H and Br-C distances for the clusters used in Figure 3.

Figure 5. Comparison of the experimental Br K-edge solution XANES spectrum with the ones obtained from the molecular dynamics simulations.

Figure 6. Several individual XANES spectra computed from snapshots of pot.C simulation (top). Averaged XANES spectrum from the same simulation including the standard deviation for the whole energy range.

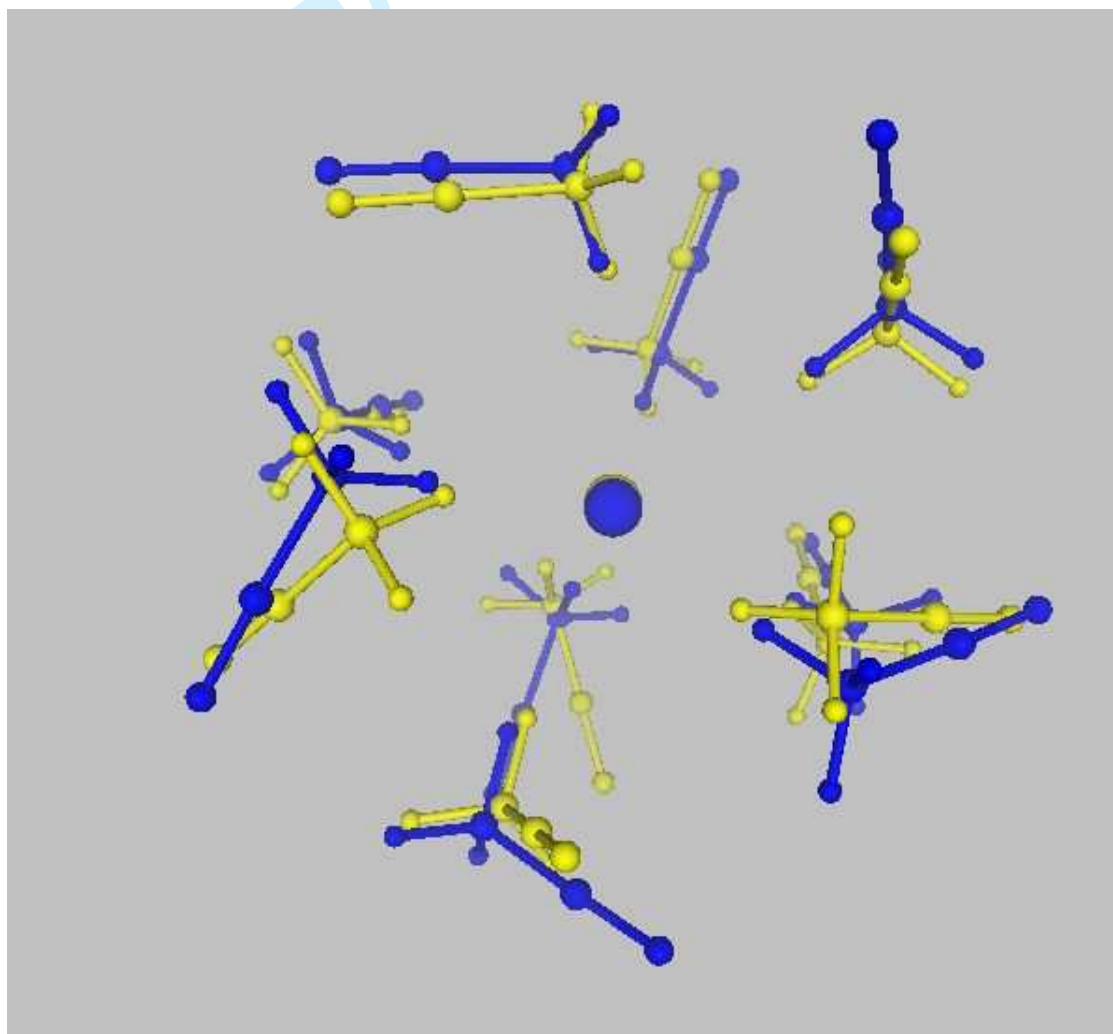


Figure 1:

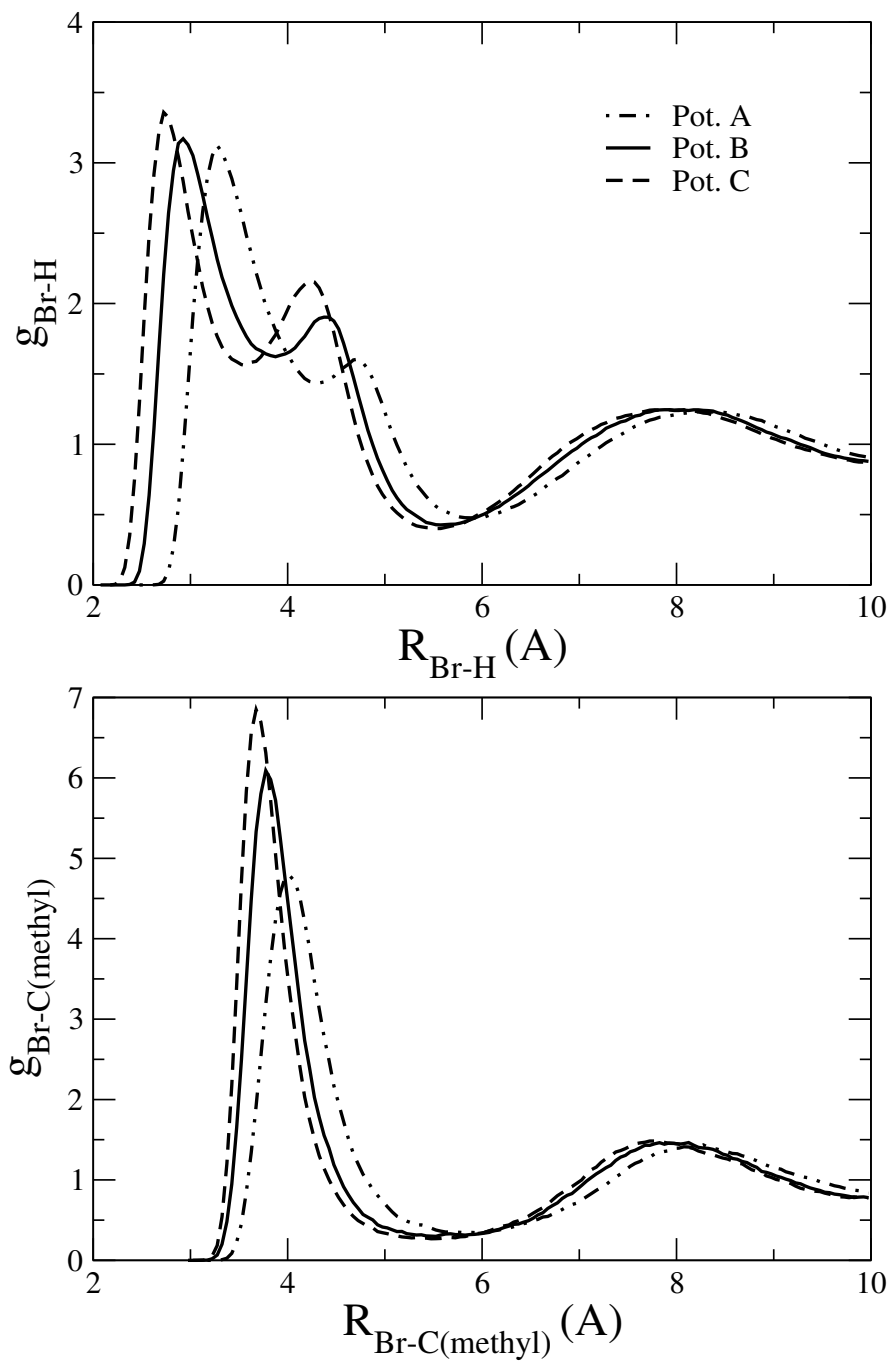


Figure 2:

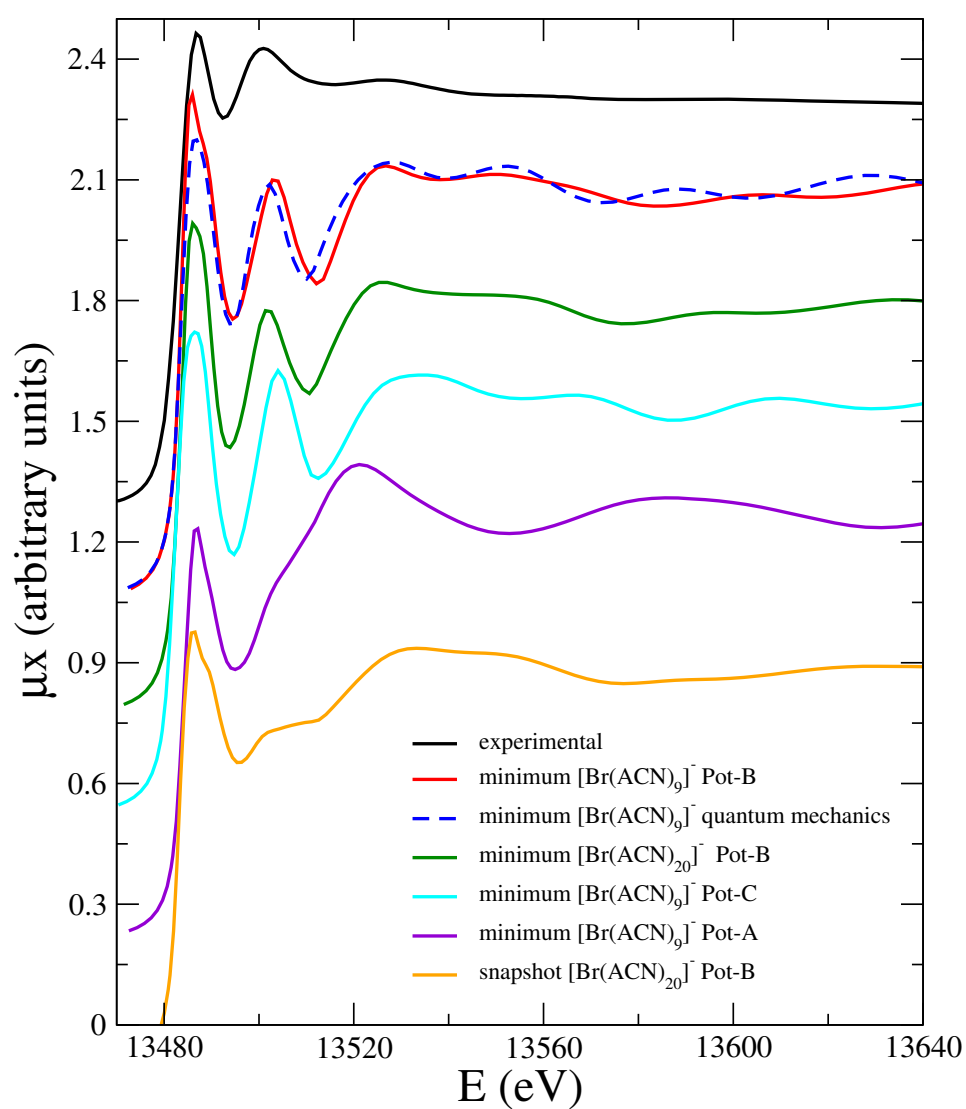


Figure 3:

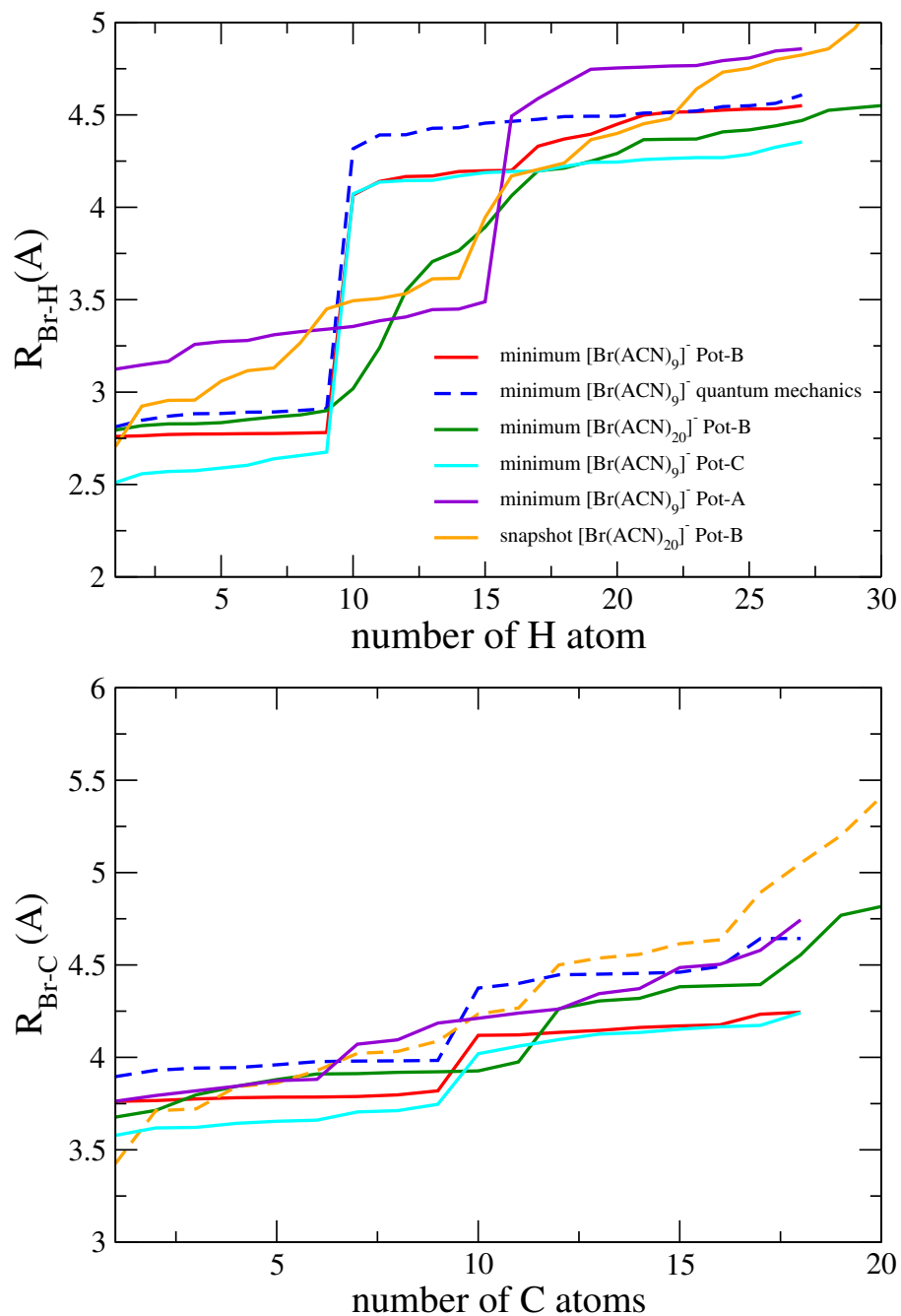


Figure 4:

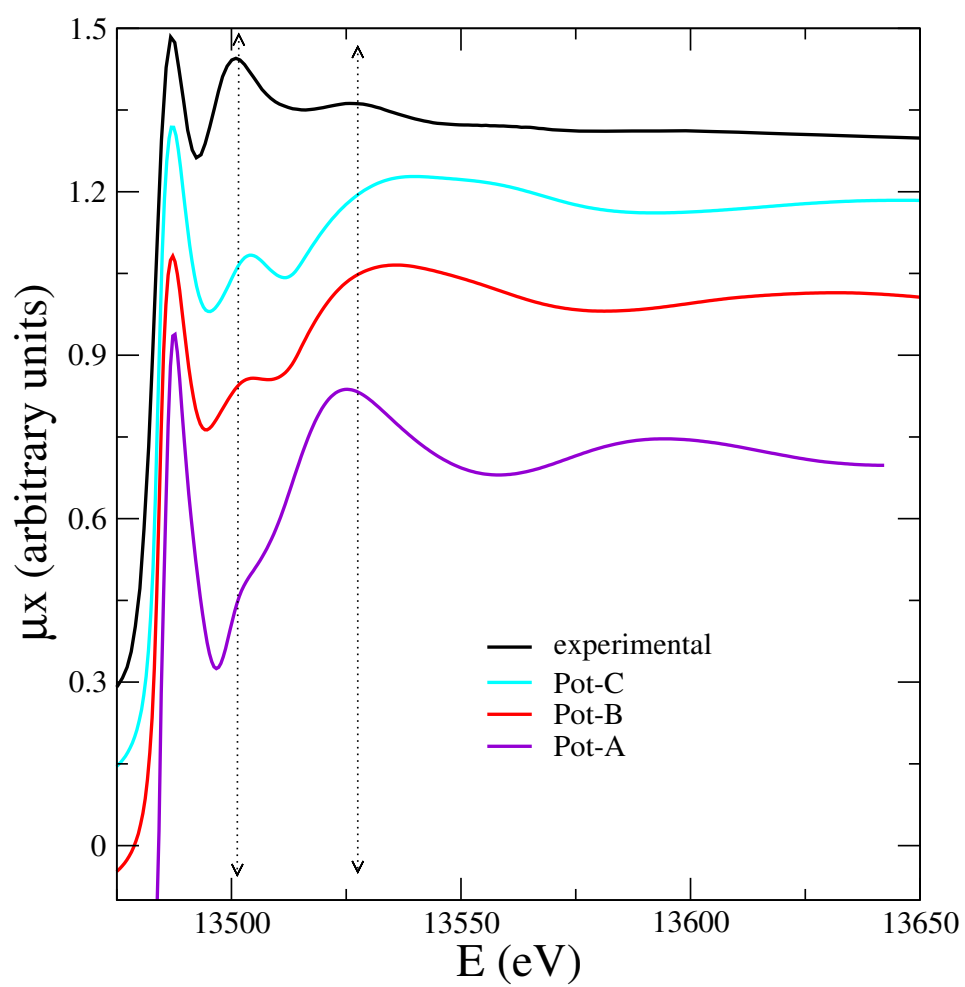


Figure 5:

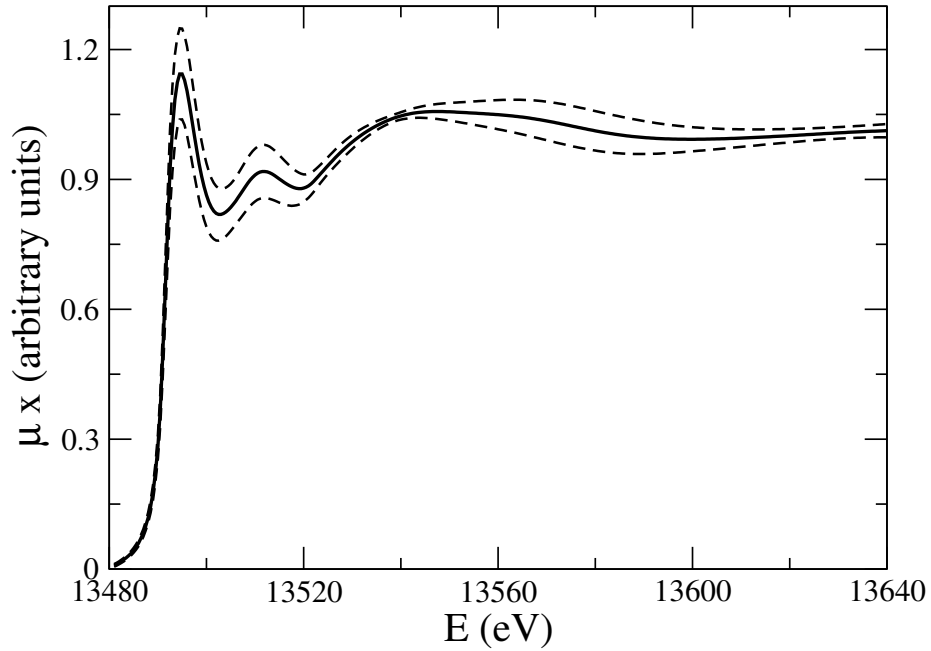
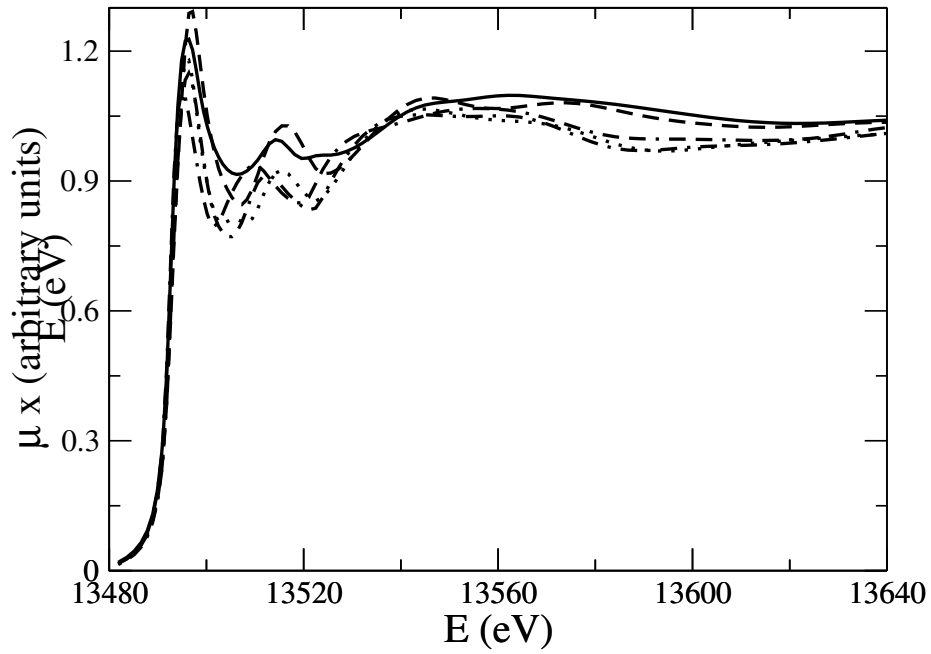
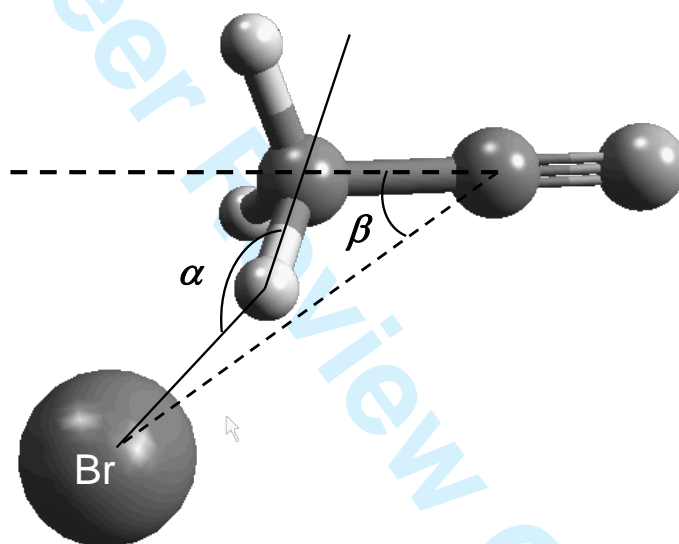


Figure 6:



Scheme 1

1
2
3
4
5
6
7
8
9
10
11
12 The Solvation of Bromide Anion in Acetonitrile: A
13
14
15
16 Structural Study Based on the Combination of
17
18
19
20 Theoretical Calculations and X-ray Absorption
21
22
23 Spectroscopy
24
25
26

27 Regla Ayala,^a José M. Martínez,^a Rafael R. Pappalardo^a

28
29 Adela Muñoz-Páez^b and Enrique Sánchez Marcos^{a,*}

30
31 (a)Departamento de Química Física and

32
33 (b)Departamento de Química Inorgánica e

34
35 Instituto de Ciencia de Materiales de Sevilla-CSIC

36
37 Universidad de Sevilla. 41012-Sevilla (Spain).

38
39 e-mail:sanchez@us.es

40
41
42
43
44
45
46
47
48
49
50
51
52
53
54
55
56
57
58
59
60
October 26, 2006

Abstract

This work studies the solvation of bromide in acetonitrile by combining quantum mechanics, computer simulations and XANES spectroscopy. Three different sets of interaction potentials were tested, one of them derived from literature and the other two are simple modifications of the previous one to include specificities of the bromide-acetonitrile interactions. Results for microsolvation of bromide were obtained by quantum mechanical optimization and classical minimization of small clusters $[\text{Br}(\text{ACN})_n]^-$ ($n=9,20$). Analysis of MD simulations has provided structural, dynamic and energetic aspects of the solvation phenomenon. The theoretical computation of Br K-edge XANES spectrum in solution using the structural information obtained from the different simulations has allowed the comparison among the three different potentials, as well as the examination of the main structural and dynamic factors determining the shape of the experimental spectrum.

1 INTRODUCTION

Although halide anions are the most common counter-ions in solution, the investigation of their solvation in aprotic solvents is very limited in comparison with that in water and other protic and polar solvents, such as alcohols.¹ This is in contrast to the increasing importance of **these types** of solutions due to their technological applications within fields such as separation chemistry, electrochemical devices or ionic recognition.¹⁻³ The non-aqueous solvation structures of halide anions are not completely defined so far owing to both experimental and theoretical difficulties. First of all, the central body of experimental data on halide solvation in non-aqueous solvents does not provide direct structural information. This is usually obtained by using reasonable models compatible with the available data. Spectroscopic and diffraction techniques offer **more** direct structural information, but the increase in the number of atom pair contributions to the global distribution function, compared to the water case, renders more difficult the structural elucidation. In addition, the high concentration of the species of interest, usually required by these techniques, does not allow **us** to discard ion-ion contributions from the global signal. For this reason, during the last decade an intense research activity on the study of small clusters has been developed with the aim of separating the ion-solvent from the pure solvent-solvent interactions.^{4,5} On the other hand, theoretical studies of halide solvation are hampered by the fact that the halide-solvent interactions are rather weak leading to a delicate balance between the ion-solvent and solvent-solvent interactions.⁶ This trend becomes particularly significant for bromide and iodide anions and for aprotic and not very polar solvents. Thus, for these two anions, solvation number within the range 1-9 are found in the literature^{2,7,8} when acetonitrile is used as solvent. Furthermore, the structural arrangement adopted by the solvent molecules is far from clear. In this sense, Richardi et al.^{3,8} propose in two theoretical studies based on Molecular Ornstein-Zernike (MOZ) theory, a non-aligned orientation of the solvent molecules with respect to the ion. This is in contrast to the conventional assumption **where** an ion-dipole interaction is dominant

1
2
3
4
5
6
7 according to which the highest stabilization energy would be provided by structures where
8 acetonitrile molecules in contact with the anion would orientate their dipole axis passing
9 through the anion center.
10
11

12
13 Nowadays, X-ray Absorption Spectroscopy (XAS) is a well-established technique to
14 study structural and electronic properties of the local environment of a given atom. A
15 large number of investigations⁹⁻¹¹ have demonstrated the suitability of this technique to
16 study ionic solutions because it requires only short-range order and can be applied to a
17 wide range of concentrations, covering several orders of magnitude (from 10^{-4} M to 10M).¹²
18 The X-ray Absorption spectrum has been traditionally divided into two energy regions.
19 The low energy part of the spectrum, extending up to $\sim 50 - 100$ eV above the absorbing
20 edge, called X-ray Absorption Near Edge Structure (XANES) region and the high energy
21 part of the spectrum (over 100 eV above the threshold up to approximately 1000 eV) called
22 Extended X-ray Absorption Fine Structure (EXAFS). The XANES region has been shown
23 to be dependent on many parameters of the system under study: the oxidation state of
24 the absorber atom, bond angles, coordination geometry, distances of the absorbing atom
25 to the **first** and higher coordination shells, etc.¹³ **Contrary** to the EXAFS region, there
26 is not a simple formulation that encompasses all these parameters. This fact has led to
27 the use of XANES information on a more qualitative level that envisages the spectrum
28 as a “fingerprint” of the system under study. In the last years, implementation of models
29 for the absorption phenomena have allowed the development of codes which accurately
30 simulate the XANES region thus approaching the situation for the EXAFS region.^{14,15} In
31 this way the theoretical simulation of XANES of ionic solutions is an emerging branch.^{16,17}
32
33

34 The aim of this work is to study the bromide solvation structure in acetonitrile by com-
35 bining the experimental information derived from XANES spectroscopy with theoretical
36 data from quantum mechanics calculations and molecular dynamics (MD) simulations.
37 For the latter ones, simple methods to get specific interaction potentials for bromide in
38 acetonitrile are investigated. The interplay of XAS spectroscopy with quantum mechanics
39
40
41
42
43
44
45
46
47
48
49
50
51
52
53
54
55
56
57
58
59
60

1
2
3
4
5
6
7 and numerical simulations has shown to be as an appropriate strategy to get insight into
8 structural information on ionic aqueous solutions,¹⁸⁻²⁷ and will be explored for the case
9 of a non-aqueous solution.
10
11

12
13 In a previous study⁶ dealing with bromide solvation within the framework of a quantum-
14 mechanical approach we showed that the bromide anion interacts with the acetonitrile
15 molecules through the hydrogen atoms of the methyl group. The linear minima are in all
16 cases slightly higher in energy than the bent ones, in good agreement with the findings of
17 Richardi et al.^{3,8} in their statistical simulation of bromide solvation in acetonitrile.
18
19
20
21
22

23
24 In this work, we will use the structural information derived from quantum chemical
25 minimizations and from statistical simulation trajectories using interactions potentials
26 from the literature^{28,29} and simple modification on them (see Section 2.2 for details) to
27 compute the XANES spectra. Direct comparison with the available experimental XANES
28 spectra for this system will allow the definition of new criteria to examine the validity of
29 the results and conclusions reached, as well as to explore an additional way to define and
30 validate intermolecular potentials.
31
32
33
34
35
36
37
38
39

40 2 COMPUTATIONAL METHODS.

41
42
43 . The analysis of the structural results derived from computations is based on the ex-
44 amination of the main features of the simulated XANES spectra and their comparison
45 with the experimental one. An input structure, as detailed as possible, is required since
46 XANES is particularly sensitive to the close environment. The source of structures to be
47 used for the simulated spectra have a double origin. First, clusters formed by one bro-
48 mide anion and an increasing number of acetonitriles molecules computed at **the** quantum
49 mechanical level. Second, snapshots extracted from the molecular dynamics trajectories
50 of a bromide anion immersed in a large number of acetonitrile molecules simulating the
51 solution, at room temperature. The computer simulations have not been limited **ex-**
52 **clusively to the application of combination rules to obtain the appropriate**
53
54
55
56
57
58
59
60

1
2
3
4
5
6
7 intermolecular potentials from the literature. In addition some easy to im-
8 plement procedures have been applied to obtain new potentials. Their validity
9 is discussed by checking the simulation results in the light of the XANES spectrum and
10 other available experimental data.
11
12
13
14

15 16 17 2.1 Quantum Mechanical Computations

18
19
20 The starting structures were taken from a previous work⁶ dealing with the microsolvation
21 of the bromide anion in water, methanol and acetonitrile. The bromide-acetonitrile
22 cluster were optimized at B3LYP level with the 6-31+G* basis set. The energy mini-
23 mized $[\text{Br}(\text{ACN})_9]^-$ structure was characterized as minimum in the PES of the bromide-
24 acetonitrile system. Gaussian03 suite of programs were used for computations.³⁰
25
26
27
28
29
30

31 32 2.2 Molecular Dynamics Simulations.

33
34
35 Three different sets of interaction potentials have been used to simulate the solvation of
36 the bromide anion in acetonitrile at room temperature (298K):
37

- 38
39 • The first set was built from the recent model of Grabuleda et al.²⁸ for acetonitrile
40 liquid, whereas bromide anion was described by the parametrization performed by
41 McCammon and col.²⁹ In both cases, potential parameters were developed in the
42 framework of the Cornell et al.³¹ force field providing flexible all-atom models for
43 the acetonitrile molecules. Internal deformations were allowed by means of the
44 usual bond, angle, and torsion terms, while the non-bonded van der Waals and
45 electrostatic terms were used to describe the intermolecular interactions. This set
46 of potentials will be labeled Pot-A (in this set of potentials, the combination rule
47 leads to a value for the van der Waals parameter of the Br-H pair $\sigma_{\text{Br-H}}=3.6 \text{ \AA}$).
48
49
50
51
52
53
54
55
56
57
58
59 • The second set of potentials tested was a simple modification of the previous one,
60 based on the hydrated ion concept developed by our group for the cation hydration

1
2
3
4
5
6
7 case.³² The solvated bromide cluster with $n=9$, $[\text{Br}(\text{ACN})_9]^-$, was used as a reference
8 structure to modify the van der Waals parameter $\sigma_{\text{Br-H}}$. For this purpose, that
9 parameter was chosen in such a way that the atomic root mean square deviation
10 (RMSD) between the quantum mechanical and force field optimized structure was
11 minimized. The optimum value was $\sigma_{\text{Br-H}} = 3.2 \text{ \AA}$ (RMSD=0.7 \AA , the superposition
12 of both structures is shown in Figure 1). This set of potentials will be labeled Pot-B.

- 13
14
15
16
17
18
19
20 • In a similar way, a third set of potentials was used by modifying the $\sigma_{\text{Br-H}}$ parameter
21 in order to test the sensitivity of the Br K-edge XANES spectrum of bromide in
22 acetonitrile to changes in the closest environment of the absorber atom, as well as
23 to other properties of the solution. Bearing in mind that the value of this parameter
24 in the first set of interaction potentials was 3.6 \AA , and 3.2 \AA for the second set, a
25 value of 2.9 \AA for $\sigma_{\text{Br-H}}$ was chosen. Thus, a range of 0.7 \AA [2.9-3.6] will be used to
26 get an insight into the relationships between spectrum and structure, on one hand,
27 and between solution properties and σ values, on the other. This set of potentials
28 will be labeled Pot-C.
29
30
31
32
33
34
35
36
37
38

39 The elementary simulation cell contained 1 bromide ion and 500 acetonitrile molecules.
40 The length of the cubic cell, $L = 30.30 \text{ \AA}$, was set to reproduce the experimental value for
41 the density of liquid acetonitrile at 25 °C. Periodic boundary conditions were applied. A
42 time step of 0.25 fs was used. The cut-off distance for the non-bonding interactions was
43 $L/2 \text{ \AA}$. **Long-range interactions were incorporated by means of Ewald summa-**
44 **tion³³ including a charged system term.^{34,35} Simulations with net charged cells**
45 **can be performed using an energy correction term which is physically equiva-**
46 **lent to adding a uniform jelly of charge that exactly neutralizes the total cell**
47 **charge.³⁶** The system was equilibrated at the chosen temperature for 50 ps, and 500
48 ps of simulation time was produced in the NVT ensemble for each set of the interaction
49 potentials considered. The average temperature was maintained constant at 300K by a
50 Berendsen thermostat³⁷ with a time constant of 0.5 ps. Structures were saved every 2
51
52
53
54
55
56
57
58
59
60

1
2
3
4
5
6
7 ps for further analysis. The MD simulations were performed with DLPOLY program,³⁸
8
9 running on a parallel multiprocessor SGI ALTIX 350 computer using 20 processors.
10

11 12 13 **2.3 Computation of XANES spectra.** 14

15
16 The K-edge XANES spectrum of bromide in acetonitrile was computed for several struc-
17
18 tures. On one hand, cluster optimized structures involving 9 acetonitrile molecules
19
20 ($[\text{Br}(\text{ACN})_9]^-$) were performed, the origin of the structures being quantum mechanically
21
22 or potential derived, as well as for a $[\text{Br}(\text{ACN})_{20}]^-$ cluster optimized with the set of in-
23
24 termolecular potentials Pot-B. On the other hand, XANES spectra obtained from MD
25
26 trajectories employing 100 snapshots equally spaced (taken every 5 ps) were also produced
27
28 for all the interaction potential sets. The final simulated XANES spectrum from the MD
29
30 simulation **corresponds** to the **average** over the spectra of each snapshot set.
31

32
33 The FEFF8.10 code program developed by Rehr's group was used to calculate the
34
35 spectra.¹⁵ The potential calculations use the Hedin-Lundqvist self-energy approxima-
36
37 tion.³⁹ A self-consistent field procedure (SCF) was employed. A 6.0 Å cutoff radius was
38
39 chosen for the SCF treatment and for the full-multiple scattering paths. A full-multiple
40
41 scattering path calculation was done taking as origin the absorber atom, i.e. the bromide
42
43 anion. Then, the chosen structure included the backscatter atoms inside a sphere of 6.0
44
45 Å radius centered at the bromide. However, for the SCF procedure, for each type of atom
46
47 the origin of the cutoff radius was placed in that atom, **which** means that the region of
48
49 the solution considered for calculation is increased by the distance between the bromide
50
51 anion and the corresponding atom. This SCF procedure introduces a difference between
52
53 the XANES computation derived from quantum mechanical or statistical calculations, as
54
55 the size of the solvent sphere surrounding the anion is, in general, not complete for all the
56
57 types of atoms when clusters optimized quantum-mechanically are considered. A XANES
58
59 spectrum calculated from 250 snapshots taken every 2 ps configurations yields very simi-
60
61 lar results to the one obtained using 100 snapshots taken every 5 ps. The consideration

of a larger cutoff radius, such as 7.0 Å in the SCF computation of the wavefunction to determine potentials and/or XANES spectra calculation do not affect the results.

In a previous work²⁷ on bromide hydration structure, it was necessary to include the hydrogen atoms to obtain a realistic backscattering potential and a simulated XANES spectrum that resembled experimental data. This could be understood by the fact that hydrogen atoms form the **closest** shell around the anion. The bromide ion induces the presence of a set of hydrogen atoms of first-shell water molecules in its closest vicinity, which are found to play a significant role in both the scattering phenomenon and in the determination of electronic wavefunctions of the bromide clusters. For the same reason, hydrogen atoms were included in the calculation of both backscattering potential and XANES spectrum in this work.

3 RESULTS AND DISCUSSION.

3.1 MD analysis.

Results of the MD analysis are summarized in Figure 2, where the Br-H and Br-C(methyl) radial distribution functions (RDFs) are plotted, and in Table 1, where a set of structural parameters, solvation energy and translational self-diffusion coefficient for the bromide anion are collected. The Br-H RDF exhibits a double peak for the first solvation shell which indicates that the three hydrogen atoms of the methyl group are not symmetrically distributed around the bromide anion. The running coordination number gives a ratio 1:2 between the two peaks, and the total number of atoms up to the second minimum (5.5-5.9 Å in Figure 2a) is around 30-33 atoms, depending on the potential set employed. These RDFs reflect the different value of the $\sigma_{\text{Br-H}}$ parameter employed. The maximum of the first peak appears at 3.28 Å for Pot-A ($\sigma_{\text{Br-H}}=3.6$ Å), at 2.93 Å for Pot-B ($\sigma_{\text{Br-H}}=3.2$ Å) and at 2.73 Å for Pot-C ($\sigma_{\text{Br-H}}=2.9$ Å). The mean angle BrHC (α) collected in Table 1 for the closest hydrogen atom to the anion is also reflecting the increasing directionality

1
2
3
4
5
6
7 of the hydrogen bond (a strong hydrogen bonding is roughly linear, i.e. an angle value
8 for XHY close to 180°): 125° for Pot-A, 135° for Pot-B and 145° for Pot-C. The asym-
9 metrical solvation of the methyl group implies that the charge(anion)-dipole(acetonitrile)
10 interaction is not the dominant contribution in the first solvation shell. Angle β defines
11 the angle formed by the molecular axis of the acetonitrile molecule and the vector formed
12 by the bromide and the center of mass of the acetonitrile molecule (Scheme 1). A β value
13 equals to 0° indicates the alignment of the anion with the molecular axis. Table 1 shows
14 that the average β value is in the range 66-80°, then the structural arrangement for the
15 first solvation agrees with the results obtained by Richardi et al.^{3,8} from MOZ theory and
16 MC simulations.

17
18
19
20
21
22
23
24
25
26
27
28 Br-C(methyl) RDFs for the three potentials are presented in Figure 2b. The maximum
29 of the first peak is found in the range 3.7-4.0Å, running integration numbers correspond
30 roughly to 10 acetonitrile molecules. The height and width of the peaks for the three po-
31 tentials show that the smaller $\sigma_{\text{Br-H}}$ is, the more compact the first solvation shell is. Exper-
32 imental estimations of coordination numbers around bromide vary in a wide range, from
33 dielectric relaxation measurements and thermodynamic data a value of 2 is obtained,^{2,7}
34 whereas from EXAFS measurements the value is close to 5.⁴⁰ This EXAFS study also
35 gives a Br-C distance of 3.48 Å which has associated **with it** a large Debye-Waller factor,
36 $\sigma^2 = (\overline{R_{\text{Br-C}} - R_{\text{Br-C}}})^2 = 0.162 \text{ \AA}^2$, implying a large static and dynamic disorder associated
37 to the Br-C parameter. When comparing these DW factors with those computed from
38 MD simulations (see Table 1), estimations are larger than the experimental one, when
39 using Pot-A a value of 0.28 Å² is obtained, whereas Pot-B and Pot-C give a similar and
40 smaller value of 0.21 Å². EXAFS equation presents a strong coupling between the coor-
41 dination number and the associated DW factors, whereas the first parameter contributes
42 to increase the intensity of the signal (the larger the number of backscatter atoms, the
43 more intense the signal becomes), the second parameter contributes to damp the intensity
44 of the signal (the larger the static and dynamic disorder around the absorber atom are,
45
46
47
48
49
50
51
52
53
54
55
56
57
58
59
60

1
2
3
4
5
6
7 less intense the signal is). Thus, for a given intensity, small values of DW factors are
8 compatible with small coordination numbers, as well as larger DW factors need larger
9 coordination numbers. The theoretical trend of the DW factors reflects that lowering the
10 $\sigma_{\text{Br-H}}$ parameter reinforces the bromide-acetonitrile interactions with respect to the MD
11 simulation with Pot-A, giving rise to tighter structures, although they are more relaxed
12 than the experimental one.
13
14
15
16
17
18

19 Regarding coordination number, Richardi et al.⁸ from their molecular Ornstein-
20 Zernike (MOZ) study predicts a value close to 9.5 molecules of acetonitrile in the first
21 solvation shell. In a later work, these authors carry out a study of halides in acetonitrile,
22 excluding bromide, comparing MOZ and **Monte Carlo** simulations.³ Maxima for the
23 first shell of X-C (X \equiv Cl and I) RDFs appear at ca. 3.8 and 4.3 Å for chloride and iodide
24 respectively, what may represent a reasonable range to enclose the Br-C distance.
25
26
27
28
29
30

31 The experimentally estimated enthalpy of solvation² is -337 kJ/mol, whereas the com-
32 puted value for the three simulations ranged between -260 and -285 kJ/mol. The sequence
33 of solvation energies for the three set of potentials follows the same order than the value of
34 $\sigma_{\text{Br-H}}$ and the corresponding distance of the first shell of acetonitrile around the halide.
35 Richardi et al.⁸ obtain similar results from their simulation when the Gibbs solvation free
36 energy is estimated, the theoretical values underestimate (provide less negative values)
37 the experimental data by 30-60 kJ/mol.
38
39
40
41
42
43
44
45

46 The translational self-diffusion coefficient for the bromide has been computed from
47 the mean-square displacement function by following the Einstein relation, theoretical D_{Br}
48 values are found to be in the range $1.4\text{-}1.6\cdot 10^{-9} \text{ m}^2\text{s}^{-1}$. There is no previous theoretical
49 estimation for D_{Br} in acetonitrile, but Guardià and Pinzon⁴¹ have computed D_{Cl} from MD
50 simulations of chloride in acetonitrile, finding a value of $1.8\cdot 10^{-9} \text{ m}^2\text{s}^{-1}$. The experimental
51 values derived from conductivity measurements are 2.66 and $2.67\cdot 10^{-9} \text{ m}^2\text{s}^{-1}$ for chloride
52 and bromide, respectively.⁴²
53
54
55
56
57
58
59
60

3.2 XANES spectra from $\text{Br}(\text{ACN})_n^-$ clusters

The usual way to relate geometrical structure around an absorber atom in a solid and features of XANES spectra is by means of the simulation of the spectrum from a reasonable geometry generally taken from crystallographic data or some related structural model. Nevertheless, when one deals with a structure in solution the source of structural information is scarce. An strategy to get advantages of both the experimental and theoretical sources of information is to simulate spectra from the structure provided by theoretical methods and to compare them with the experimental spectra. A synergy may be established, such that theoretical procedures could be improved by approaching the computed spectrum to the experimental one, and simultaneously the structural information derived from the spectrum is refined, and the features of the spectra properly assigned.

First of all, we are going to compare the XANES spectra obtained for clusters formed by one bromide anion and a number of acetonitrile molecules small enough to define only the first solvation shell $[\text{Br}(\text{ACN})_9]^-$, subsequently, the first and second solvation shells will be included, $[\text{Br}(\text{ACN})_{20}]^-$, and both spectra compared. Figure 3 includes comparative plots of the experimental spectrum obtained by Watanabe and col.⁴⁰ with those computed for the optimized structures $[\text{Br}(\text{ACN})_9]^-$ obtained by applying the three sets of potentials and the quantum mechanical level. The spectra obtained from the structures derived quantum mechanically by using Pot-B and Pot-C present the three main resonances and their relative intensities are quite similar to the experimental spectrum. On the contrary, Pot-A derived structure leads to a quite different ratio of intensities which makes the computed spectrum rather different in shape from the experimental one, even though resonances appears at the same energy values. The spectrum derived from the structure optimized quantum-mechanically has been over-imposed to that derived of Pot-B to show the sensitivity of XANES features to small changes, since the fitted $\sigma_{\text{Br-H}}$ value was chosen just to bring the potential-derived structure containing nine acetonitrile molecules as close as possible to quantum-mechanical one. (The RMS for the structure was 0.7 Å,

1
2
3
4
5
6
7 and Figure 1 shows the similarity between both structures). The changes that a second
8 solvation shell induces on the spectrum features can be observed in the XANES generated
9 for the $[\text{Br}(\text{ACN})_{20}]^-$ cluster (obtained through the use of Pot-B). The comparison with
10 the nona-acetonitrilated cluster for Pot-B suggests that second-shell effects are marginal:
11 a small change in the relative intensities of the three resonances and a slight smoothing,
12 both at the white line and at the high-energy part of the spectrum. It is worth noting
13 that the computed spectra show more intense features at the high energy region than the
14 experimental one. This is a consequence of the rigidity and symmetry of the structures
15 used, since their origin is an energy minimization. In contrast, the spectrum obtained for a
16 cluster of 20 acetonitrile molecules but whose structure is a snapshot of the MD trajectory
17 with Pot-B is smeared out and the intensity of the second resonance is reduced.

18
19
20
21
22
23
24
25
26
27
28
29
30 To show the relationships between XANES features and structure around bromide,
31 Figure 4 plots the distribution of the distances for the two first types of backscatter atoms
32 surrounding the halide, that is hydrogen and carbon atoms of acetonitrile molecules.
33 Ordinate contains the corresponding distance of the backscatter atoms to the bromide
34 whereas abscissa gives the order number established on the basis of the H(or C)-Br dis-
35 tance. Thus, the curve $R_{\text{Br-H}}$ vs. n_{H} for the minimum $[\text{Br}(\text{ACN})_9]^-$ structure obtained
36 quantum-mechanically shows nine H atoms placed at 2.79-2.90 Å. The additional 18 hy-
37 drogen atoms of the cluster are placed at larger distances within the range 4.30-4.60Å.
38 The structure obtained by Pot-A exhibits the most distant first shell of H atoms, located
39 in between the two previous ranges of distances (3.2-3.5 Å) and with almost a double
40 number of backscatters (15). Its XANES spectrum is that differing most from the exper-
41 imental one. An intermediate distribution is shown by the snapshot with 20 molecules,
42 where $R_{\text{Br-H}}$ values increases monotonically, although the closest distances are more sim-
43 ilar to the two minimum geometries obtained with Pot-B. In the case of the optimized
44 cluster with 20 solvent molecules using the set of potentials B, the shape of the spectrum
45 is more similar to the corresponding structure with 9, indicating that the second set of
46
47
48
49
50
51
52
53
54
55
56
57
58
59
60

1
2
3
4
5
6
7 H atoms play a minor role on the XANES features. It is worth pointing out that the
8
9 sequence of Br-H distance for Pot-C, Pot-B and quantum mechanics compared with the
10
11 energy gap between the two first resonances illustrates pretty well the Natoli's rule,¹³
12
13 i.e. the difference in energy between the white line and the energy of a given feature is
14
15 inversely proportional to the coordination distance of the shell of atoms related with this
16
17 feature. The Br-C distributions show a sequence of distances for the first shell of atoms
18
19 which differs from that obtained for the Br-H one. Thus, the quantum mechanical cluster
20
21 bears the longest $R_{\text{Br-C}}$ for the seven closest C atoms to Br. The $[\text{Br}(\text{ACN})_9]^-$ clusters
22
23 for Pot-B, Pot-C and quantum mechanics level, as well as the $[\text{Br}(\text{ACN})_{20}]^-$ for Pot-B
24
25 retains similar shape of $R_{\text{Br-C}}$ distributions than the R_{BrH} ones. There is a plateau of
26
27 $R_{\text{Br-C}}$ for the first shell of C atoms which denotes the consistency of the shell in these
28
29 simulations. In fact this pattern, which is defined by a regular coordination sphere of C
30
31 atoms placed at quite similar distance of bromide, seems to be the most direct contri-
32
33 bution to the XANES features. In particular, the intensity of the second resonance and
34
35 the relative height of the white line with respect to the second resonance are affected by
36
37 the $R_{\text{Br-C}}$ value and the symmetry of its distribution. This is observed when the XANES
38
39 spectrum is computed for two modified structures of the quantum mechanic $[\text{Br}(\text{ACN})_9]^-$
40
41 minimum, where selectively the Br-C distance is changed by +0.1 and -0.1 Å.
42
43

44 As previously remarked in the literature,^{16,25,26,43} these findings show that for the
45
46 XANES definition **the geometrical arrangement of atoms around the photo-**
47
48 **absorber is essential**, such that slightly different structures could lead to clearly different
49
50 spectra.
51
52

53 3.3 XANES spectra from MD simulations.

54
55
56 The computed Br K-edge XANES spectrum of bromide in acetonitrile solution at 298K
57
58 obtained from MD simulations which used the three different set of potentials are shown
59
60 in Figure 5. In contrast with the structure of clusters, these spectra are the average

1
2
3
4
5
6
7 for a large number of structures (100 snapshots) which result from the fluctuations of
8 the solvent structure around the bromide. The relevance of the changes induced by
9 the fluctuation might be seen either by individual inspection of spectra corresponding
10 to several snapshots or by drawing the standard deviation of the absorption line along
11 the whole energy range. These two plots have been included in Figure 6. The individual
12 XANES spectra coming from different snapshots show significant differences among them,
13 specially at low energy. The interesting fact derived from this figure is that the majority
14 of the individual spectra are quite different to the average. This stresses the importance
15 of carrying out a thorough sampling of the configurational space to properly compute the
16 XANES spectra in solution. This is not surprising if one bears in mind the differences
17 **found** in the XANES features when using the different clusters studied in the previous
18 section. Similar results were found in an earlier theoretical-experimental study on the
19 hydration of bromide.²⁷ Geometrical fluctuations **generate** quite different local hydration
20 environments around bromide, then leading to quite different shape of spectra derived by
21 each individual snapshot (for instance see Figure 2 in ref [27]).

22
23
24
25
26
27
28
29
30
31
32
33
34
35
36
37
38 As shown in Figure 5, the spectrum computed from the MD snapshots of Pot-A gives
39 a rather poor reproduction of the experimental spectrum, something that was already
40 observed for the minimized structure using this potential (Figure 3). The other two
41 spectra are more similar to the experimental one, although in both cases the relative
42 intensity of the second resonance decreases with respect to the simulated XANES obtained
43 with their corresponding optimized clusters (Figure 3). On the contrary, the global shape
44 of these spectra are smoother compared to the non-statistically averaged spectra obtained
45 for the clusters. Thus, the tail of the XANES is smeared out in contrast to the XANES
46 computed for clusters and the global spectrum is damped by the statistical average.
47 Considering the magnitude of the deviations of the individual spectra with respect to the
48 averaged one, **the similarity among the experimental spectra and those obtained**
49 **from the cluster structures (quantum mechanics or classical potentials, Pot-**
50
51
52
53
54
55
56
57
58
59
60

1
2
3
4
5
6
7 **B and Pot-C)** could be surprising because the clusters ones are based on an
8 **unique structure which correspond with the minimum for each cluster size.**
9
10
11 Nevertheless, there is a fundamental difference between the snapshots and the structures
12 derived **from** an energy minimization. The latter ones are the direct consequence of the
13 balanced interaction potentials operating in the system (represented by a cluster of a given
14 size) and, on this basis they could be considered as single representative configurations.
15
16
17 When solvation of a monoatomic ion is considered, a relatively small region of the solvent
18 around the ion is perturbed by it, so that the microscopic picture could be envisaged
19 as that of an ionic cluster immersed in a pure solvent. The short-range sensitivity of
20 the XANES spectroscopy implies that a cluster of a few angströms around the ion is
21 responsible **for** the spectrum shape. When the ion-solvent interactions are stronger than
22 the solvent-solvent ones, the fluctuations of the solvent molecules in the closer environment
23 of the ion (and simultaneously the absorber atom) are small and an averaged structure
24 may be representative of the ion solvation shells. Even more, strong attractive interactions
25 around the ion promotes a quite harmonic behavior of the ion-solvent interactions in
26 this region which generates averaged structures quite consistent with those corresponding
27 to the potential energy minimizations. The comparison of experimental and computed
28 XANES indicates that the main features of the spectrum are pretty well reproduced by
29 some of the energy optimized clusters, that is, these structures are representative ones,
30 although the fluctuations included by the averaging of snapshots is needed to smear out
31 the whole spectrum.
32
33
34
35
36
37
38
39
40
41
42
43
44
45
46
47
48
49

50
51 When comparing the distribution of distances for the first **backscatterers** of bro-
52 mide in the clusters (Figure 3) and the peak of the corresponding RDF in Figure 2, a
53 shift appears in the Br-H distance of about 0.18 Å from the optimized clusters Pot-B and
54 Pot-C to their first maxima in Br-H RDF (**2.75Å to 2.93Å for Pot-B and 2.55Å to**
55 **2.73Å for Pot-C**), in addition to wide peaks that allows a significant range of asym-
56 metric arrangements compatible with the dynamic of the system. This shifting indicates
57
58
59
60

1
2
3
4
5
6
7 that solvent effects and/or temperature effects induces a significant relaxation of the first
8 solvation shell for the set of potentials Pot-B and Pot-C, where the bromide-acetonitrile
9 interactions may become stronger in the first shell. **The main geometrical feature**
10 **changing with $\sigma_{\text{Br-H}}$ when going from structures of minimum for clusters in**
11 **gas phase to solution is just the Br-H distance. The interactions between the**
12 **solvated ion and bulk solvent and those between the solvent-solvent molecules**
13 **play a role equivalent to an increase of this parameter, $\sigma_{\text{Br-H}}$. This is one of**
14 **the reasons that make the computed XANES derived from MD simulation**
15 **with Pot-C more similar to the experimental one. The solvent effects on the**
16 **Br-C distances are much smaller in these two simulations compared with the**
17 **cluster minima (from 3.75Å to 3.78Å for Pot-B and from 3.62Å to 3.68Å for**
18 **Pot-C), which indicates a decrease of the orientational angles α and β (See**
19 **Scheme 1).**

20
21
22
23
24
25
26
27
28
29
30
31
32
33 It is interesting to notice that previous studies on cation hydration²⁴⁻²⁶ following the
34 same methodology have shown that the mismatch between individual spectra and the
35 averaged one is less important than that observed in the anion solvation.²⁷ The reason is
36 that anion-solvent interactions are weaker than the cation-solvent ones. Additional factors
37 derived from simulation contribute to modify the shape of the spectrum whose detailed
38 analysis can not be easily split. A general conclusion is that for the set of potentials em-
39 ployed, the acetonitrile-acetonitrile interactions are too much dominant with respect to the
40 bromide-acetonitrile ones. Provided that acetonitrile simulations of the pure solvent gives
41 consistent results,²⁸ a strategy to improve the description of the bromide solution could be
42 to define a more attractive bromide-acetonitrile interaction potential by including in the
43 fitting ab initio interaction energies of clusters, in addition to geometrical criteria. Like-
44 wise, as pointed out by Richardi et al.³ for the case of aprotic solvents, or by Ayala et al.⁴⁴
45 for the case of water, the consideration of a polarizable model certainly must introduce
46 some improvements in the detailed balance among the ion-solvent and solvent-solvent in-
47
48
49
50
51
52
53
54
55
56
57
58
59
60

1
2
3
4
5
6
7 interactions. The results derived from simulations are consistent with previous simulations
8
9 of related systems, using other intermolecular potentials and/or computational modeling,
10
11 such as integral equations or Monte Carlo.¹
12

13 14 15 **4 Concluding Remarks.** 16

17
18 Simulations of bromide in acetonitrile have been carried out by means of the use of
19
20 interaction potentials available in the literature, and simple modifications of them based
21
22 on structural criteria associated to the hydrated ion concept.
23

24
25 The structural description of the local environment of bromide anion in acetonitrile is
26
27 a rather relaxed first solvation shell formed by ca. 10 acetonitrile molecules where one of
28
29 the hydrogen atoms of the methyl group is placed closer to the anion, 2.7-2.9 Å, than the
30
31 other two hydrogen atoms of the methyl group (ca. 4.2-4.4 Å) due to the bent orientation
32
33 of the acetonitrile molecules (**approx.** 130 °) with respect to the bromide anion. This
34
35 allows the carbon atom of the methyl group to be closer to the bromide, ca. 3.7-3.8 Å.
36
37 A small second peak at 8 Å shows a quite diffuse shell that is more dominated by the
38
39 acetonitrile solvent structure than by the anion.
40

41
42 Taken into account that different theoretical approaches have been employed as source
43
44 of structural information, several solvation environment around the bromide have been
45
46 described, allowing us a detailed analysis of the relationship between structures, XANES
47
48 features and static and dynamic disorder of the solution. Given the difficulty of estab-
49
50 lishing a direct relation with other observables in solution, XANES (and EXAFS) has
51
52 revealed as an interesting guide to validate or improve computer simulations. In this
53
54 particular case, it has been shown that the coordination shells beyond the first one do
55
56 not make an important contribution to the spectrum.
57

58
59 The resemblance between the theoretical spectra obtained from quantum mechanically
60
optimized clusters ($n \geq 9$) and the average spectra derived from MD simulations with
some of the set of potentials allows us to conclude that those clusters are a good model

1
2
3
4
5
6
7 picture of the structure of bromide in acetonitrile. Nonetheless, the discrepancies among
8 the individual spectra derived from MD simulations indicate that this representation
9 should be taken as an average model picture with important standard deviations. The
10 set of potential called Pot-B seems the most appropriate to deal with small clusters of
11 $[\text{Br}(\text{ACN})_n]^-$ (for $n \geq 20$), whereas the set Pot-C seems the more convenient to describe
12 acetonitrile solutions containing bromide.
13
14
15
16
17
18
19
20

21 **5 Acknowledgments**

22 This work was supported by Spanish DGICYT (CTQ2005-03657). **We thank Prof. I.**
23 **Watanabe (Osaka University) for supplying the EXAFS experimental data of**
24 **the bromide anion in acetonitrile. His interesting comments and suggestions**
25 **are also acknowledged.**
26
27
28
29
30
31
32
33
34
35
36
37
38
39
40
41
42
43
44
45
46
47
48
49
50
51
52
53
54
55
56
57
58
59
60

References

1. Barthel, J. M. G.; Krienke, H.; Kunz, W. *Physical Chemistry of Electrolyte Solutions*; Steinkopff: Darmstadt, 1998.
2. Marcus, Y. *Ion Solvation*; Wiley: Chichester, 1985.
3. Fischer, R.; Richardi, J.; Fries, P. H.; Krienke, H. *J. Chem. Phys.* **2002**, *117*, 8467.
4. Markovich, G.; Cheshnovsky, O.; Perera, L.; Berkowitz, M. L. *J. Chem. Phys.* **1996**, *105*, 2675.
5. Megyes, T.; Radnai, T.; Wakisaka, A. *J. Mol. Liq.* **2003**, *103-104*, 319.
6. Ayala, R.; Martínez, J. M.; Pappalardo, R. R.; Sánchez Marcos, E. *J. Phys. Chem. A* **2000**, *104*, 2799.
7. Barthel, J.; Kleebauer, M.; Buchner, R. *J. Solution Chem.* **1995**, *24*, 1.
8. Richardi, J.; Fries, P. H.; Krienke, H. *J. Chem. Phys.* **1998**, *108*, 4079.
9. Koningsberger, D. C.; Prins, R., Eds.; *X-Ray Absorption: Principles, Applications, Techniques of EXAFS, SEXAFS, and XANES*; Wiley: New York, 1988.
10. Ohtaki, H.; Radnai, T. *Chem. Rev.* **1993**, *93*, 1157.
11. Richens, D. T. *The Chemistry of Aqua Ions*; John Wiley: Chichester, 1997.
12. Muñoz-Páez, A.; Pappalardo, R.; Sánchez Marcos, E. *J. Am. Chem. Soc.* **1995**, *117*, 11710.
13. A. Bianconi, X-Ray Absorption: Principles, Applications, Techniques of EXAFS, SEXAFS and XANES. In ; Koningsberger, D. C.; Prins, R., Eds.; John Wiley: New York, 1988.

- 1
2
3
4
5
6
7 14. Natoli, C. R.; Benfatto, M.; Brouder, C.; Ruiz López, M. F.; Foulis, D. L. *Phys.*
8 *Rev. B* **1990**, *42*, 1944.
9
10
11 15. Ankudinov, A.; Ravel, B.; Rehr, J. J.; Conradson, S. D. *Phys. Rev. B* **1998**, *58*,
12 7565.
13
14
15 16. Benfatto, M.; Solera, J. A.; Chaboy, J.; Proietti, M. G.; García, J. *Phys. Rev. B*
16 **1997**, *56*, 2447.
17
18
19 17. Díaz-Moreno, S.; Muñoz-Páez, A.; Chaboy, J. *J. Phys. Chem. A* **2000**, *104*, 1278.
20
21
22 18. Palmer, B. J.; Pfund, D. M.; Fulton, J. L. *J. Phys. Chem.* **1996**, *100*, 13393.
23
24
25 19. Roccatano, D.; Berendsen, H. J. C.; D'Angelo, P. *J. Chem. Phys.* **1998**, *108*, 9487
26 and references therein.
27
28
29 20. Filipponi, A.; D'Angelo, P.; Pavel, N. V.; Di Cicco, A. *Chem. Phys. Lett.* **1994**,
30 225, 150.
31
32
33 21. Spångberg, D.; Hermansson, K.; Lindqvist-Reis, P.; Jalilehvand, F.; Sandström, M.;
34 Persson, I. *J. Phys. Chem. B* **2000**, *104*, 10467.
35
36
37 22. Jalilehvand, F.; Spångberg, D.; Lindqvist-Reis, P.; Hermansson, K.; Persson, I.;
38 Sandström, M. *J. Am. Chem. Soc.* **2001**, *123*, 431.
39
40
41 23. Campbell, L.; Rehr, J. J.; Schenter, G. K.; McCarthy, M. I.; Dixon, D. *J. Syn-*
42 *chrotron Radiat.* **1999**, *6*, 310.
43
44
45 24. Merklings, P. J.; Muñoz-Páez, A.; Martínez, J. M.; Pappalardo, R. R.; Sánchez
46 Marcos, E. *Phys. Rev. B* **2001**, *64*, 012201.
47
48
49 25. Merklings, P. J.; Muñoz-Páez, A.; Pappalardo, R. R.; Sánchez Marcos, E. *Phys. Rev.*
50 *B* **2001**, *64*, 092201.
51
52
53
54
55
56
57
58
59
60

- 1
2
3
4
5
6
7 26. Merklings, P. J.; Muñoz-Páez, A.; Sánchez Marcos, E. *J. Am. Chem. Soc.* **2002**, *124*,
8 10911.
9
10
11 27. Merklings, P. J.; Ayala, R.; Martínez, J.; Pappalardo, R.; Sanchez Marcos, E. *J.*
12 *Chem. Phys.* **2003**, *119*, 6647.
13
14
15 28. Grabuleda, X.; Jaime, C.; Kollman, P. A. *J. Comput. Chem.* **2000**, *21*, 901.
16
17
18 29. Lybrand, T. P.; Ghosh, I.; McCammon, J. A. *J. Am. Chem. Soc.* **1985**, *107*, 7793.
19
20
21 30. Frisch, M. J.; Trucks, G. W.; Schlegel, H. B.; G. E. Scuseria, M. A. R.; et. al.,
22 *Gaussian 03*; Gaussian, Inc.: Wallingford CT, 2004.
23
24
25 31. Cornell, W. D.; Cieplak, P.; Bayly, C. I.; Gould, I. R.; Merz, K. M.; Fergus-
26 son, D. M.; Spellmeyer, D. C.; Fox, T.; Caldwell, J. W.; Kollman, P. A. *J. Am.*
27 *Chem. Soc.* **1995**, *117*, 5179.
28
29
30 32. Martínez, J.; Pappalardo, R. R.; Sánchez Marcos, E. *J. Am. Chem. Soc.* **1999**, *121*,
31 3175.
32
33
34 33. Allen, M. P.; Tildesley, D. J. *Computer Simulation of Liquids*; Oxford University
35 Press: Oxford, 1987.
36
37
38 34. Leslie, M.; Gillan, M. J. *J. Phys.: Cond. Matter* **1985**, *18*, 973.
39
40
41 35. Roberts, J. E.; Schnitker, J. *J. Phys. Chem.* **1995**, *99*, 1322.
42
43
44 36. Figueirido, F.; Del Buono, G. S.; Levy, R. M. *J. Chem. Phys.* **1995**, *103*, 6133-6142.
45
46
47 37. Berendsen, H.; Postma, J.; van Gusteren, W.; DiNola, A.; Haak, J. *J. Chem. Phys.*
48 **1984**, *81*, 3684.
49
50
51 38. Smith, W.; Forester, T. R. "DL-POLY 2.13", 1996.
52
53
54 39. Hedin, L.; Lundqvist, S. *Solid State Phys.* **1969**, *23*, 1.
55
56
57
58
59
60

- 1
2
3
4
5
6
7 40. Sawa, Y.; Miyanaga, T.; Tanida, H.; Watanabe, I. *J. Chem. Faraday Trans.* **1995**,
8 *91*, 4389.
9
10
11 41. Guardià, E.; Pinzón, R. *J. Mol. Liquids* **2000**, *85*, 33.
12
13
14
15 42. Krumgalz, B. S. *J. Chem. Soc. Faraday Trans. 1* **1983**, *79*, 571.
16
17
18 43. D'Angelo, P.; Benfatto, M.; Della Longa, S.; Pavel, N. V. *Phys. Rev. B* **2002**, *66*,
19 0642091.
20
21
22
23 44. Ayala, R.; Martínez, J.; Pappalardo, R.; Saint-Martin, H.; Ortega-Blake, I.;
24 Sánchez Marcos, E. *J. Chem. Phys.* **2002**, *117*, 10512.
25
26
27
28
29
30
31
32
33
34
35
36
37
38
39
40
41
42
43
44
45
46
47
48
49
50
51
52
53
54
55
56
57
58
59
60

Table 1. MD Results

Potentials	Structural Results				
	$R_{max}(g_{Br-H})(\text{\AA})$	$R_{max}(g_{Br-C(methyl)})(\text{\AA})$	$\sigma_{Br-C}^2 (\text{\AA}^2)$	$\bar{\alpha} (\text{\textcircled{C}})$	$\bar{\beta} (\text{\textcircled{C}})$
A	3.28	4.01	0.28	125	66
B	2.93	3.78	0.21	135	77
C	2.73	3.68	0.21	145	80
	$E_{solv}(\text{kJ mol}^{-1})$		$D (10^{-9} \text{ m}^2 \text{ s}^{-1})$		
A	-259.2.		1.6±0.1		
B	-275.9		1.6±0.1		
C	-284.5		1.4±0.1		

Figure legends.

Figure 1. Quantum Mechanically optimized structure (blue) for $[\text{Br}(\text{ACN})_9]^-$ cluster together with the minimum RMSD configuration (yellow) according to the $\sigma_{\text{Br}-\text{H}}$ parameter (see text for details).

Figure 2. Radial distribution functions for Br-H and Br-C(methyl) pairs of pot.A, pot.B and pot.C simulations.

Figure 3. Experimental Br K-edge XANES spectrum (black) and theoretically simulated spectra for different bromide-acetonitrile clusters.

Figure 4. Br-H and Br-C distances for the clusters used in Figure 3.

Figure 5. Comparison of the experimental Br K-edge solution XANES spectrum with the ones obtained from the molecular dynamics simulations.

Figure 6. Several individual XANES spectra computed from snapshots of pot.C simulation (top). Averaged XANES spectrum from the same simulation including the standard deviation for the whole energy range.

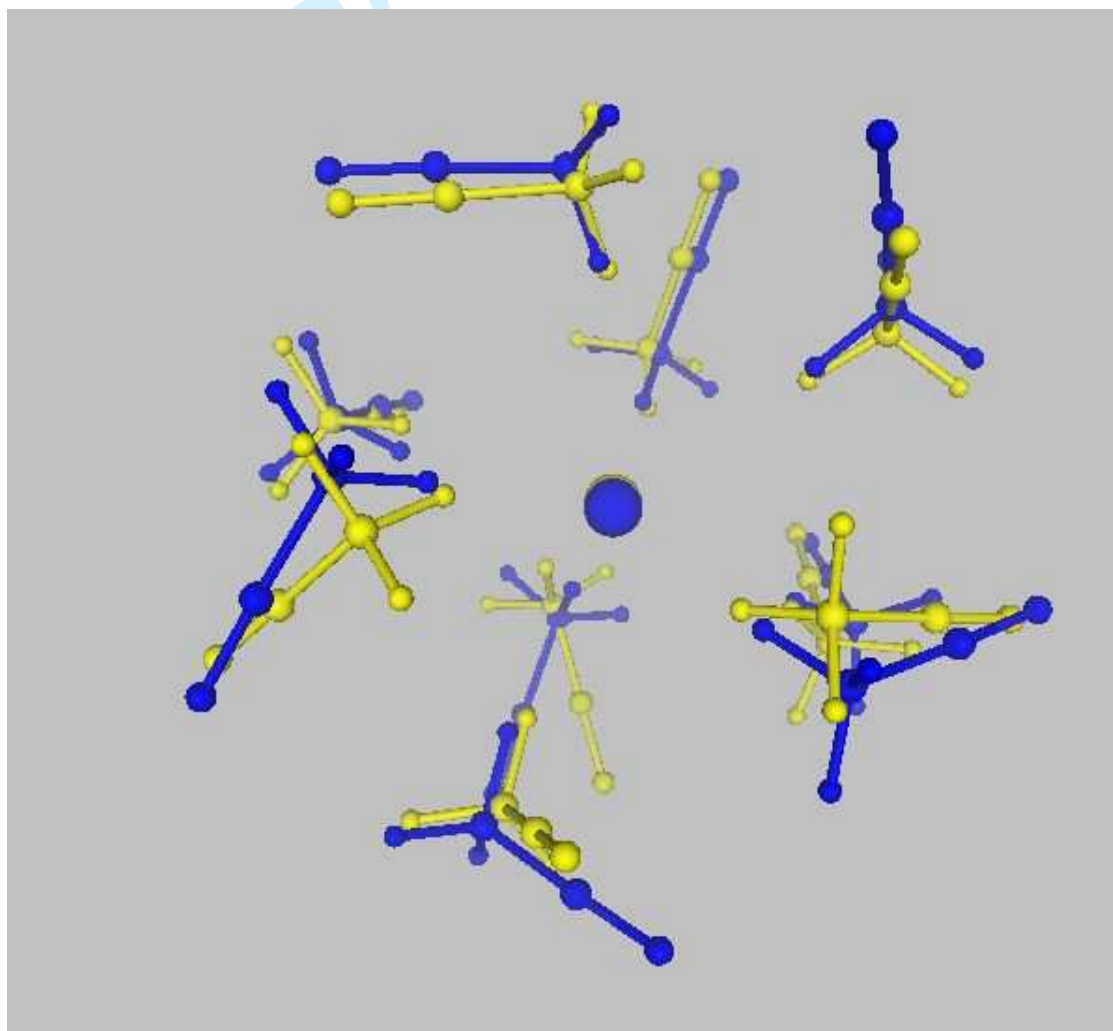


Figure 1:

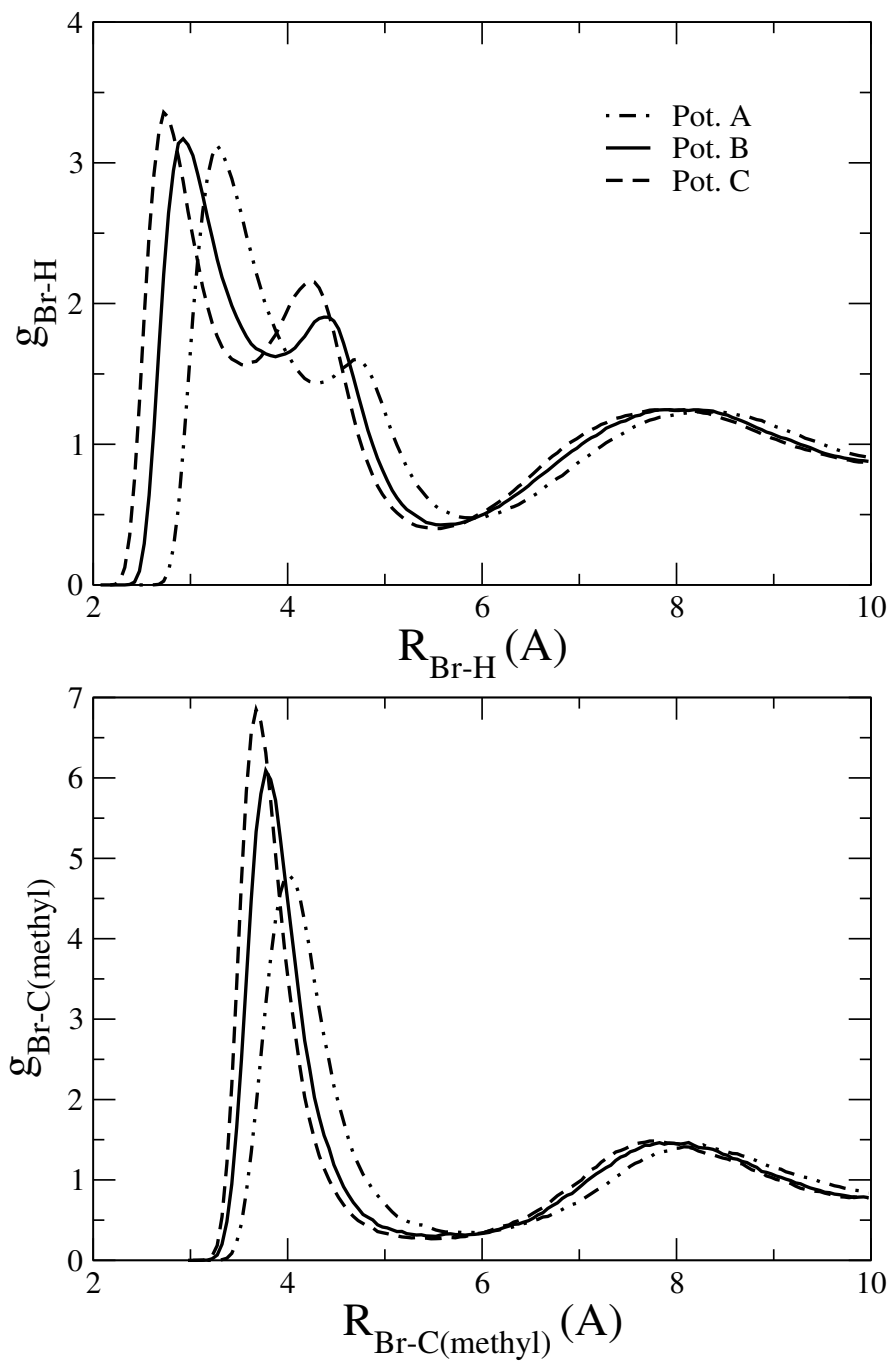


Figure 2:

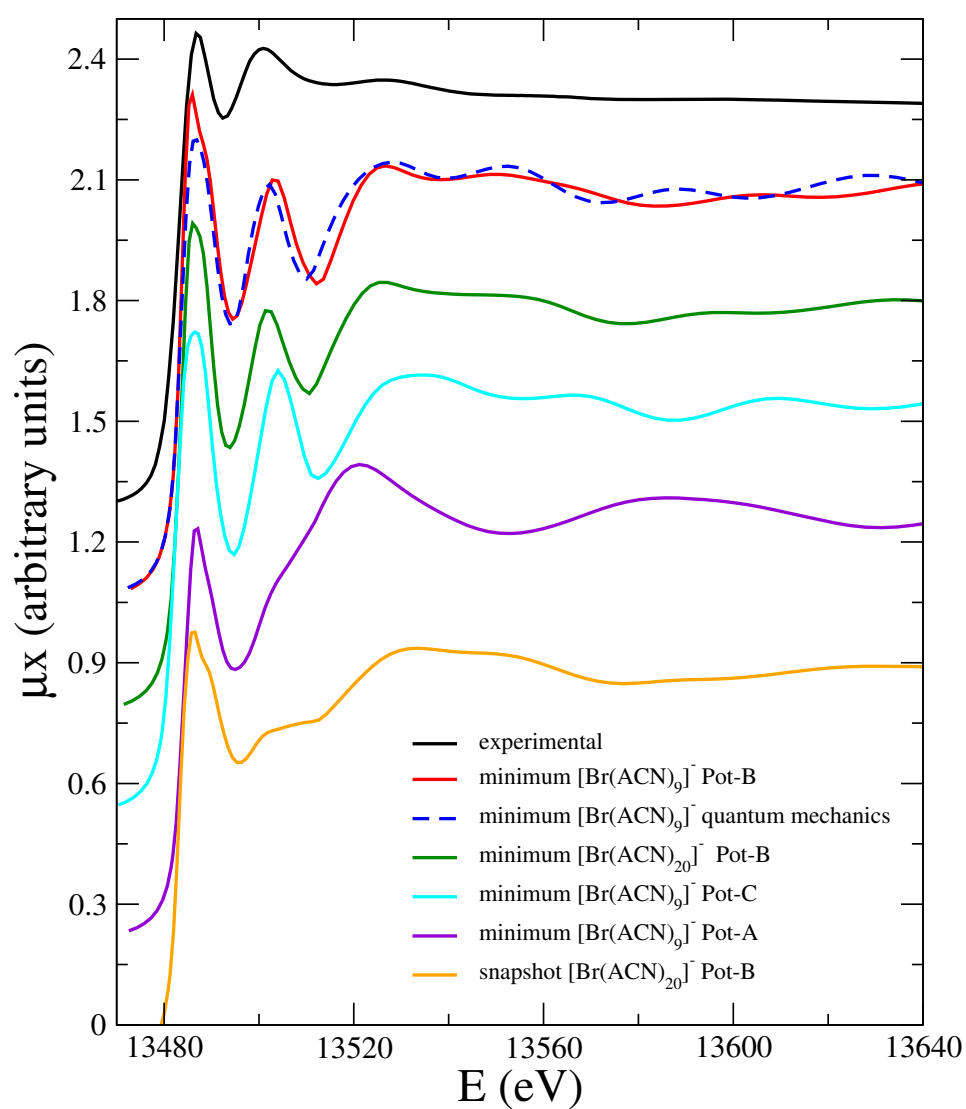


Figure 3:

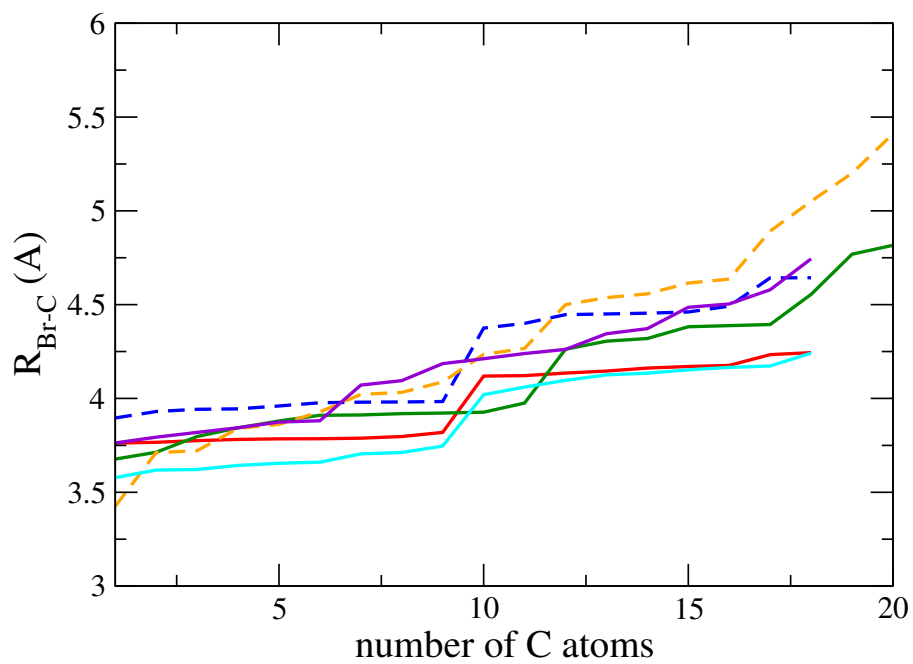
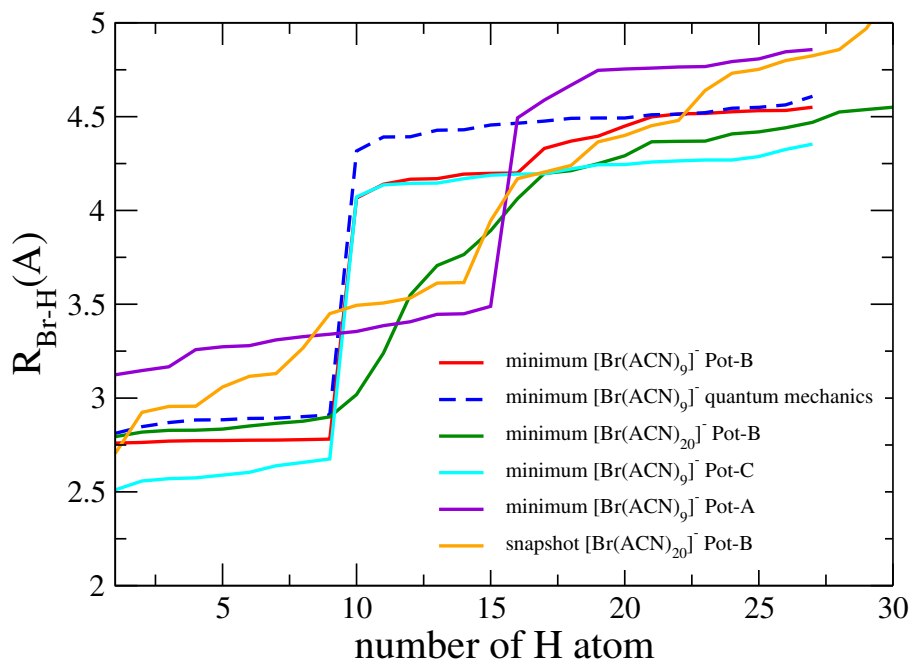


Figure 4:

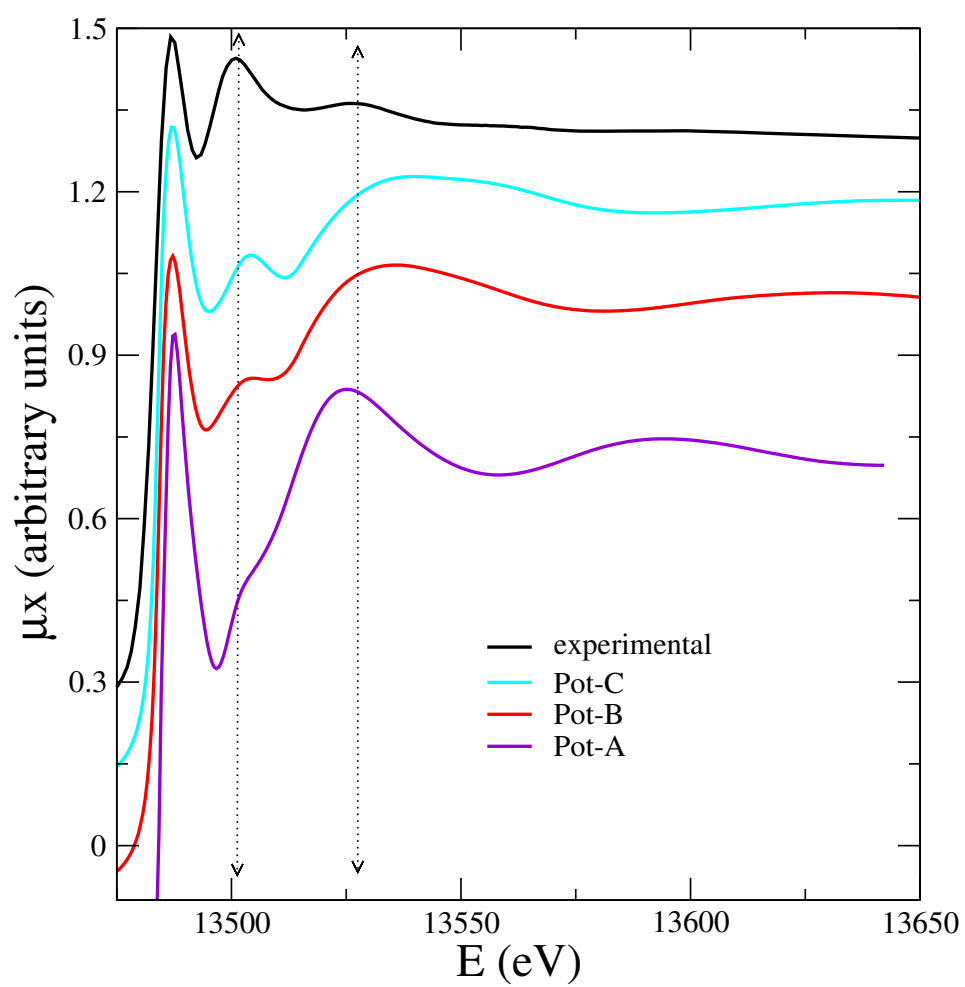


Figure 5:

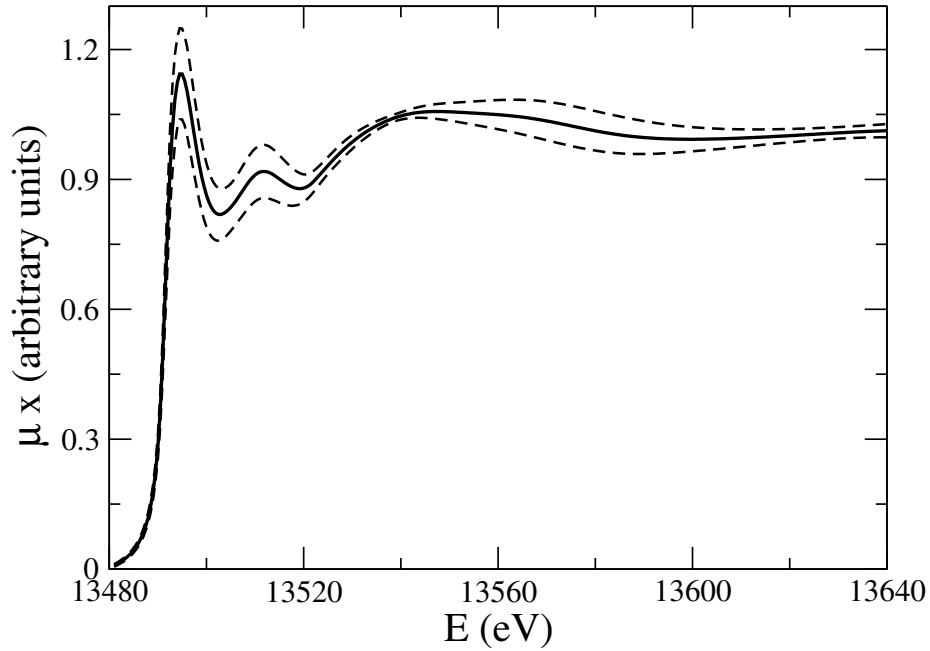
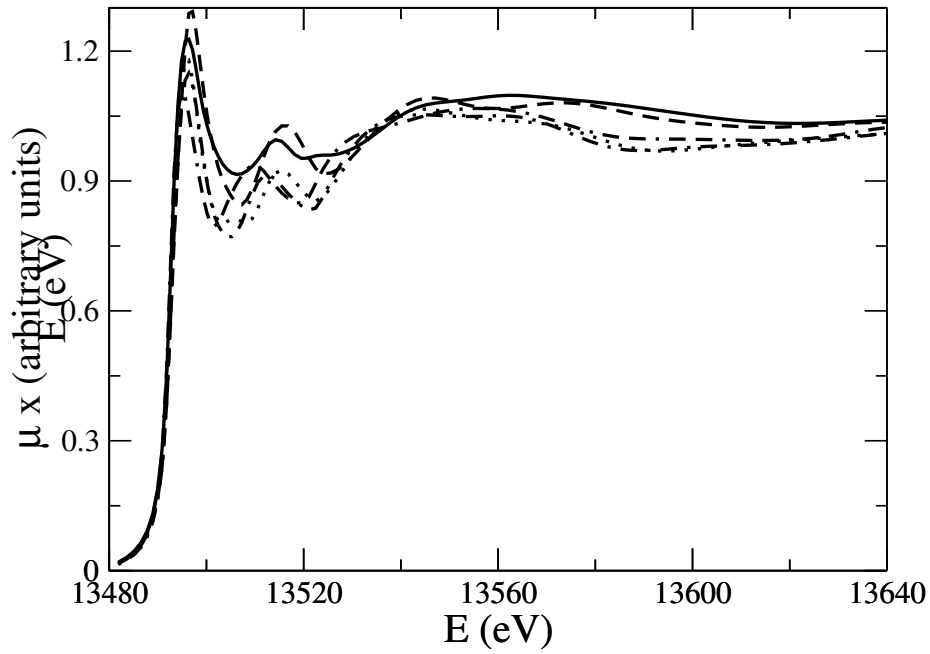
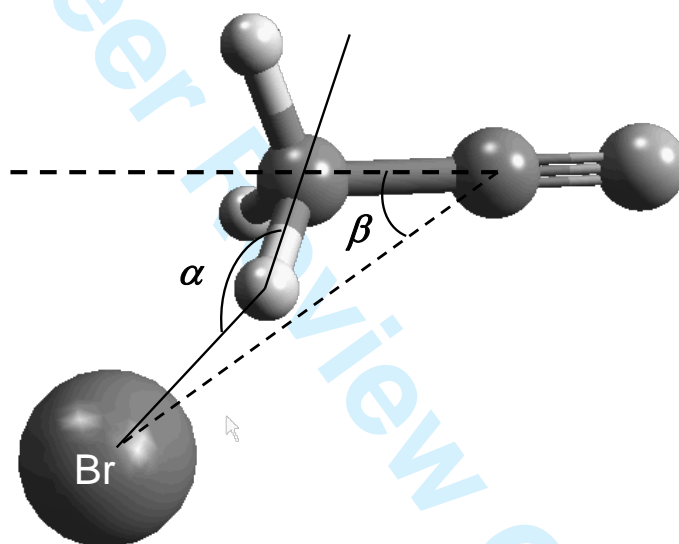


Figure 6:



Scheme 1